Relic Gravitational Waves as a Source of CMB Polarization

Kasemets, Tomas

Published in:
LU TP 08-03

2008

LU TP 08-03
February 29, 2008

RELIC GRAVITATIONAL WAVES AS A SOURCE OF CMB POLARIZATION

Tomas Kasemets

Bachelor Thesis in Theoretical High Energy Physics,
Department of Theoretical Physics, Lund University,
Sölvegatan 14A, SE 223 62 Lund, Sweden

Supervisor: Johan Bijnens

Abstract

The effect of relic gravitational waves on the polarization of the CMB is analytically studied. The equation of radiative transfer for the polarization is transformed into two coupled differential equations by Polnarev's method and an approximate solution is derived.

Contents

1 Introduction **4**

2 Preliminaries **5**
2.1 Stokes Parameters 5
2.2 The Goal of Calculations 6
2.3 Thomson Scattering as a Source of Polarization 6
2.4 Relic Gravitational Waves 6

3 Full Sky Analysis **8**
3.1 Living on the Sphere 8
3.2 Polarization on the Sphere 9

4 The Boltzmann Equation **11**

5 Power Spectra and Correlation Functions **14**
5.1 Expanding the Solutions 14
5.2 Polarization Power Spectra 15

6 Time Evolution of RGWs **16**

7 Visibility Function **21**

8 Solving the Boltzmann Equation **22**

9 Results and Discussion **28**
9.1 The Effect of the Visibility Function 29
9.2 The Dependence on Tensor/Scalar Ratio 30
9.3 Dependence on the Baryon Density 31
9.4 Location of the Peaks 34
9.5 Influence of the spectrum index 34

10 Conclusions **39**

A Appendix **39**
A.1 Transverse-Traceless Gauge 39
A.2 Base Functions for Thomson Scattering 40
A.3 Sachs-Wolfe Effect 41
A.4 Coupled Differential Equations 43
A.4.1 Unperturbed Radiation 43
A.4.2 Perturbed Radiation 43
A.5 Curl and Divergence of Spherical Harmonics 46
A.6 Expansion Coefficients 47
A.6.1 The Electric Type 48
A.6.2 The Magnetic Type 50
A.7 Solution to RGWs Equation of Motion 51

A.7.1 Radiation Era 51
A.7.2 Matter Era 52
A.8 Sudden Transition Approximation 53
A.9 Tight Coupling Expansion 54
A.9.1 Zero Order 54
A.9.2 First Order 55
A.9.3 Second Order 55

B Second Order Approximation **56**

1 Introduction

Fluctuations of the Cosmic Microwave Background (CMB) caused by gravitational waves will be studied analytically in this paper. This will be done in the first order approximation of the metric perturbations caused by the relic gravitational waves.

In the early universe photons were tightly coupled to matter by Thomson scattering. As the universe expanded and cooled down to about 3000 K, protons and electrons formed neutral Hydrogen. The baryon and photon fluids decoupled and the last scattering occured. Since then these photons have essentially been decoupled from baryons, meaning that the radiation from last scattering has been left intact. Therefore the CMB provides a picture of the universe at last scattering and a way to examine the early stages of our universe.

A temperature map of the CMB shows small temperature fluctuations and has confirmed one of the predictions of inflationary big bang theories, where a period of rapid expansion follows the bang. The quantum fluctuations are enlarged and cause inhomogeneities in the universe. One way to test inflationary theories and indirectly detect gravitational waves is to measure the polarization of the CMB. Polarization can originate from temperature inhomogeneities through Thomson scattering but also from metric perturbations, both scalar and tensorial. The tensorial part is caused by gravitational waves and are the main focus of this thesis. The polarization induced by tensorial perturbations is of lower magnitude than the scalar induced, but gives rise to a different kind of polarization, the magnetic type, and can also be important for the electric type in long wavelengths.

Cosmic shear (gravitational lensing) can interfere with the picture of the universe at last scattering by displacing the CMB. If the gravitational waves have been strong enough they can be detected without correcting for this effect, and if not, there are ways of subtracting the effect of cosmic shear [2]. The effects of reionization and free streaming neutrinos have not been included. Reionization will cause another peak in the visibility function, giving another peak in the polarization power spectra while the neutrinos could cause a damping, slightly lowering the spectra.

The organization of this thesis is as follows. In the second section some background material is presented, such as the Stokes parameters, Thomson scattering and relic gravitational waves (RGWs). The third section introduces some consepts of a spherical manifold. In the fourth section the equation of radiative transfer (The Boltzmann equation or BE) is introduced to describe the time evolution of the polarization. In the fifth section the power spectra is obtained in terms of the Legendre expansion of the solution to the BE. Before actually solving the Boltzmann equation the visibility function, section six, and the time evolution of the RGWs, section seven, are needed. Finally, in section eight, the BE for the polarization is solved to the second order of the tight coupling and the result is used to obtain the two types of polarization power spectra. Thereafter follows a section with results and examination of the effect of different parameters, such as the tensor to scalar ratio and the speed of the

decoupling. The conclusions can be found in section 10. Appendix A contain some rather lengthy derivations while appendix B discuss the differences between the results of this theisis and the one in [1], while including the second order approximation of the tight coupling.

I have mainly used two papers, *Analytic approach to the CMB polarization generated by relic gravitational waves* by W. Zhao and Y. Zhang [1], and *Theory of cosmic microwave background polarization* by P. Cabella and M. Kamionkowski [2]. *Cosmic microwave background fluctuations from gravitational waves: An analytic approach* by J.R. Pritchard and M. Kamionkowski [9] has been important in my attempts to comprehend.

I have done all intermediate steps in the analytical calculations of [1] and I have analytically reproduced most results of [1].

2 Preliminaries

2.1 Stokes Parameters

The polarization of an electromagnetic wave can be described by the four Stokes parameters (I, Q, U, V). Where I is the intensity, Q and U are linear-polarization parameters and V is a circular-polarization parameter.

The electric-field vector of a monochromatic wave propagating in the $\hat{z}$-direction is

$$\mathbf{E} = E_x\hat{x} + E_y\hat{y} = \left(a_x e^{i\delta_x}\hat{x} + a_y e^{i\delta_y}\hat{y}\right) e^{i(kz-\omega t)} \tag{1}$$

and the Stokes parameters are then

$$\begin{cases} I = |E_x|^2 + |E_y|^2 \\ Q = |E_x|^2 - |E_y|^2 \\ U = 2\Re(E_x E_y^*) \\ V = 2\Im(E_x E_y^*) \end{cases}. \tag{2}$$

If the coordinate system is rotated by and angle δ, the Stokes parameters transform as

$$\begin{aligned} I' &= |E'_x|^2 + |E'_y|^2 = |\cos\delta E_x + \sin\delta E_y|^2 + |-\sin\delta E_x + \cos\delta E_y|^2 \\ &= I, \qquad (3) \\ Q' &= |E'_x|^2 + |E'_y|^2 = |\cos\delta E_x + \sin\delta E_y|^2 + |-\sin\delta E_x + \cos\delta E_y|^2 \\ &= (\cos^2\delta - \sin^2\delta)(|E_x|^2 - |E_y|^2) + 2\sin\delta\cos\delta(E_x E_y^* + E_x^* E_y) \\ &= \cos 2\delta Q + \sin 2\delta U, \qquad (4) \\ U' &= 2\Re(E'_x E'^*_y) = -\sin 2\delta(|E_x|^2 - |E_y|^2) + 2\Re\cos 2\delta E_x E_y^* \\ &= -\sin 2\delta Q + \cos 2\delta U, \qquad (5) \\ V' &= 2\Im(E'_x E'^*_y) = 2\Im\cos 2\delta E_x E_y^* = V. \qquad (6) \end{aligned}$$

I and V are invariant while Q and U transform as

$$\begin{pmatrix} Q' \\ U' \end{pmatrix} = \begin{pmatrix} \cos 2\delta & \sin 2\delta \\ -\sin 2\delta & \cos 2\delta \end{pmatrix} \begin{pmatrix} Q \\ U \end{pmatrix} \tag{7}$$

or equivalently when

$$x' = A_i^k x_k \tag{8}$$

then

$$P_{ij} = \begin{pmatrix} Q & -U \\ -U & -Q \end{pmatrix} \tag{9}$$

transforms as

$$P'_{ij} = A_i^k A_j^l P_{kl}. \tag{10}$$

This means that Q and U transform as the components of a symmetric traceless 2×2 tensor, i.e. a spin-2 field [2]. Therefore the linear polarization can be given a rotationally invariant description by the tensor, P_{ij}.

2.2 The Goal of Calculations

The aim is to calculate the polarization tensor, $P_{ab}(\hat{n})$ and use this to get the power spectra caused by the RGWs. We consider ourselves sitting in the center of a sphere (earth), and measuring the polarization of the infalling radiation from all directions (the surface of the sphere or the sky). The polarization map created from experiments can then be used to obtain the correlation functions and then the polarization power spectrum.

2.3 Thomson Scattering as a Source of Polarization

When electromagnetic radiation scatters on a charge particle, the electric and magnetic components of the wave will accelerate the particle and thereby cause it to emit radiation. The polarization of this scattered light will depend on both the polarizations of the infalling light and the differences in intensities from different directions. [2]

Radiation falling in on an electron in the y and x directions can be scattered in the z direction. The scattered radiation will have the x part of the polarization from the incoming y direction and the y part of the polarization from the radiation incoming in the x direction, fig. 1. If the infalling radiation from the two directions have different intensity and/or is polarized the scattered radiation will be linearly polarized.

The observation of small temperature fluctuations in the background radiation implies a temperature difference in different regions of the early universe and thus, the radiation from different parts must have differed in intensity and the scattered light will be polarized.

Since Thomson scattering does not induce any phaseshift, it will never produce any circular polarization, so $V = 0$.

2.4 Relic Gravitational Waves

Another cause of polarization of the CMB is Relic Gravitational Waves, caused by the quantum fluctuations in the early, dense universe. The polarization

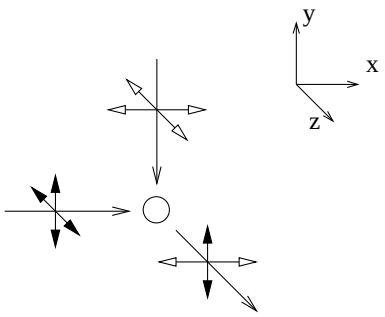

Fig. 1: Radiation incident along the x and y axes scatter against an electron causing a polarization in the radiation scattered along the z axis.

from the perturbation of the metric is different from that caused by temperature anisotropies and scalar perturbations. The perturbed flat Friedmann-Robertson-Walker metric is

$$ds^2 = a^2(\eta)\left[d\eta^2 - (\delta_{ij} + h_{ij})dx^i dx^j\right], \tag{11}$$

where η is the conformal time and the size of the horizon

$$\eta = \int \frac{a_0(t)}{a(t)} dt, \tag{12}$$

h_{ij} are perturbations with $|h_{ij}| << 1$, $a(\eta)$ is the scale factor. The perturbations can be both scalar and tensorial but it is only the tensorial type that originates from the RGWs [1].

The RGWs are symmetric and using the gauge freedom to choose the transverse traceless gauge it is seen that there can only be two independent types of gravitational waves, h^+_{ij} and $h^\times_{ij}$ (A.1). An arbitrary gravitational wave can be described as a superposition of plane waves. The problem is, to first order, linear in the perturbations and therefore the polarization and anisotropy generated by a gravitational wave is the superposition of the polarization generated by plane waves. This allows for the study of one plane gravitational wave and then summarize in the end to get the total effect of arbitrary gravitational waves. Choosing a gravitational wave propagating in the z-direction, the perturbations can be described by

$$h_{ij} = h^+_{ij} + h^\times_{ij} = h^+\epsilon^+_{ij} + h^\times\epsilon^\times_{ij}, \tag{13}$$

where

$$\epsilon^+_{ij} = \begin{pmatrix} 1 & 0 & 0 \\ 0 & -1 & 0 \\ 0 & 0 & 0 \end{pmatrix} \tag{14}$$

and

$$\epsilon_{ij}^{\times} = \begin{pmatrix} 0 & 1 & 0 \\ 1 & 0 & 0 \\ 0 & 0 & 0 \end{pmatrix}. \tag{15}$$

Taking the normal spherical coordinates where θ is the polar angle and ϕ is the azimuthal angle, defining $\mu = \cos\theta$ the cartesian coordinate vectors are

$$\hat{n}_x = (1-\mu^2)^{1/2}\cos\phi \tag{16}$$
$$\hat{n}_y = (1-\mu^2)^{1/2}\sin\phi \tag{17}$$

in the (μ, ϕ) base, leading to

$$\epsilon_{ij}^{+}\hat{n}_i\hat{n}_j = (1-\mu^2)\cos 2\phi \tag{18}$$
$$\epsilon_{ij}^{\times}\hat{n}_i\hat{n}_j = (1-\mu^2)\sin 2\phi. \tag{19}$$

3 Full Sky Analysis

The CMB reach us from every direction of the sky and in order to analyse the experimentally measured polarization over the full sky and to compare it with computational, numerical or analytical, results, the curvature of the 2-sphere has to be taken into account. Therefore this section introduces some of the mathematical properties and how they are implemented in the calculations of the polarization power spectra and correlation functions.

3.1 Living on the Sphere

The curvature of the 2-sphere is described by the metric

$$g_{ab} = \begin{pmatrix} 1 & 0 \\ 0 & \sin^2\theta \end{pmatrix}. \tag{20}$$

The covariant derivatives is denoted by (:). For a scalar field

$$S_{:a} = S_{,a}, \tag{21}$$

for a vector field

$$V^a{}_{:b} = V^a{}_{,b} + V^c\Gamma^a_{bc} \tag{22}$$

and for a tensor field

$$T^{ab}{}_{:c} = T^{ab}{}_{,c} + T^{db}\Gamma^a_{cd} + T^{ad}\Gamma^b_{cd}, \tag{23}$$

where the Christoffel symbols are

$$\Gamma^a_{bc} = \frac{1}{2}g^{ad}(g_{db,c} + g_{dc,b} - g_{bc,d}). \tag{24}$$

Any symmetric trace free rank-2 tensor can be written as the gradient of one scalar field A

$$A_{:ab} - \frac{1}{2} g_{ab} A^{:c}_{c} \tag{25}$$

and the curl of another scalar field B

$$\frac{1}{2}(B_{:ac}\epsilon^{c}{}_{b} + B_{:bc}\epsilon^{c}{}_{b}), \tag{26}$$

where

$$\epsilon_{ab} = \sin\theta \begin{pmatrix} 0 & 1 \\ -1 & 0 \end{pmatrix} \tag{27}$$

is the antisymmetric tensor. Any scalar field on the sphere can be expanded in spherical harmonics. Thus any 2-tensor on the 2-sphere can be expanded in the complete orthonormal set of curl and divergence of spherical harmonics,

$$Y^{G}_{(lm)ab} = N_l \Big(Y_{(lm):ab} - \frac{1}{2} g_{ab} Y_{(lm):c}{}^{c} \Big), \tag{28}$$

$$Y^{C}_{(lm)ab} = \frac{N_l}{2} \Big(Y_{(lm):ac}\epsilon^{c}_{b} + Y_{(lm):bc}\epsilon^{c}{}_{a} \Big). \tag{29}$$

The normalization factor,

$$N_l = \sqrt{2(l-2)!/(l+2)!} = \sqrt{2(l+2)(l+1)l(l-1)}, \tag{30}$$

is chosen so that

$$\int d\hat{n} Y^{X*}_{(lm)ab}(\hat{n}) Y^{X'\,ab}_{(l'm')}(\hat{n}) = \delta_{ll'}\delta_{mm'}\delta_{XX'}, \tag{31}$$

where $(X, X') = \{G, C\}$. [2]

3.2 Polarization on the Sphere

The symmetric trace free polarization tensor, eq. 9, for the full sky in spherical coordinates $\hat{n} = (\theta, \phi)$ is

$$P_{ab}(\hat{n}) = \frac{1}{2} \begin{pmatrix} Q(\hat{n}) & -U(\hat{n})\sin\theta \\ -U(\hat{n})\sin\theta & -Q(\hat{n})\sin^2\theta \end{pmatrix}, \tag{32}$$

where the $\sin\theta$ factors originates from that the basis of the two-sphere (θ, ϕ) is not normalized [2]. Expanding the polarization tensor in the divergence and curl of spherical harmonics,

$$\frac{P_{ab}(\hat{n})}{T_0} = \sum_{l=2}^{\infty} \sum_{m=-l}^{l} \Big[a^{G}_{(lm)} Y^{G}_{(lm)ab}(\hat{n}) + a^{C}_{(lm)} Y^{C}_{(lm)ab}(\hat{n}) \Big]. \tag{33}$$

T_0 is the average temperature of the CMB and the coefficients of the expansion $a^G_{(lm)}$ and $a^C_{(lm)}$, represent the electric and magnetic (divergence and curl) components of the polarization [1]. The $l = \{0, 1\}$ equals zero so they can be left out of the sum. The expansion coefficients are given by

$$a^G_{(lm)} = \frac{1}{T_0}\int d\hat{n} P_{ab}(\hat{n}) Y^{G\,ab*}_{(lm)}(\hat{n}), \tag{34}$$

$$a^C_{(lm)} = \frac{1}{T_0}\int d\hat{n} P_{ab}(\hat{n}) Y^{C\,ab*}_{(lm)}(\hat{n}). \tag{35}$$

The polarization power spectra are defined as

$$\langle a^{X*}_{(lm)} a^{X'}_{(l'm')}\rangle = C_l^{XX'}\delta_{ll'}\delta_{mm'}, \tag{36}$$

where the brackets indicate expectation value, or the average over all realizations [2]. For a given l the sum over m runs from $-l$ to l containing $2l + 1$ terms. The coefficients give us the electric and magnetic type of power spectrum. After measuring the polarization of the entire sky, the results can be used to get a polarization map and calculate the correlation functions. The value of the correlation between two points will depend on the coordinate system and therefore the coordinates are always chosen so that one axis is parallel and one perpendicular to the great arc connecting the two points. When calculating the correlation function on the two-sphere, because of the spherical symmetry, one of the points can be chosen freely and ϕ can be put to zero. It is convenient to choose the north pole as one of the points and θ is then the parameter of the great arc connecting the poles. Taking $Q(0, 0)$ to be the limit when θ tends to zero, the cross-correlation functions are defined as

$$C^{QQ}(\theta) = \left\langle \frac{Q(0,0)}{T_0}\frac{Q(\theta,0)}{T_0}\right\rangle \tag{37}$$

and

$$C^{UU}(\theta) = \left\langle \frac{U(0,0)}{T_0}\frac{U(\theta,0)}{T_0}\right\rangle. \tag{38}$$

With the expansion of the polarization tensor, eq. 33, Stokes parameters Q and U are

$$Q(\theta,\phi) = T_0\sum_{l=2}^{\infty}\sum_{m=-l}^{l} N_l\left[a^G_{(lm)}W_{(lm)} - a^C_{(lm)}X_{(lm)}\right] \tag{39}$$

and

$$U(\theta,\phi) = -T_0\sum_{l=2}^{\infty}\sum_{m=-l}^{l} N_l\left[a^G_{(lm)}X_{(lm)} + a^C_{(lm)}W_{(lm)}\right] \tag{40}$$

where $W_{(lm)}(\theta, \phi)$ and $X_{(lm)}(\theta, \phi)$ are defined in (A.5). $W_{(lm)}(0, 0)$ and $X_{(lm)}(0, 0)$ differ from zero only when $m = \pm 2$,

$$W_{(lm)} = \frac{1}{2}\sqrt{\frac{2l+1}{4\pi}\frac{(l+2)!}{(l-2)!}}(\delta_{m,2} + \delta_{m,-2}) \tag{41}$$

and

$$X_{(lm)} = \frac{i}{2}\sqrt{\frac{2l+1}{4\pi}\frac{(l+2)!}{(l-2)!}}(\delta_{m,2} - \delta_{m,-2}). \tag{42}$$

Thus the correlation functions are

$$\begin{aligned} C^{QQ}(\theta) &= \left\langle \frac{Q(0,0)}{T_0}\frac{Q(\theta,0)}{T_0} \right\rangle \\ &= \sum_{lml'm'} N_l N_{l'} \Big\langle \left[a^G_{(lm)} W_{(lm)}(0,0) - a^C_{(lm)} X_{(lm)}(0,0)\right] \\ &\quad \times \left[a^{G*}_{(l'm')} W^*_{(l'm')}(\theta,0) - a^{C*}_{(l'm')} X^*_{(l'm')}(\theta,0)\right] \Big\rangle. \\ &= \sum_{lml'm'} a^G_{(lm)} \sqrt{\frac{2l+1}{8\pi}} N_{l'} \left\langle a^G_{(lm)} a^{G*}_{(l'm')} \right\rangle (\delta_{m,2} + \delta_{m,-2}) W^*_{(lm)} \\ &\quad + \left\langle a^C_{(lm)} a^G_{(l'm')} \right\rangle (\delta_{m,2} - \delta_{l,-2}) X^*_{(lm)} \\ &= \sum_l \sqrt{\frac{2l+1}{8\pi}} N_l \left[C^{GG}_l (W^*_{l,2} + W^*_{l,-2}) + iC^{CC}_l (X^*_{l,2} - X^*_{l,-2})\right] \end{aligned} \tag{43}$$

and similarly

$$\begin{aligned} C^{UU}(\theta) &= \left\langle \frac{U(0,0)}{T_0}\frac{U(\theta,0)}{T_0} \right\rangle \\ &= \sum_{lml'm'} N_l N_{l'} \Big\langle \left[a^G_{(lm)} X_{(lm)}(0,0) + a^C_{(lm)} W_{(lm)}(0,0)\right] \\ &\quad \times \left[a^{G*}_{(l'm')} X^*_{(l'm')}(\theta,0) + a^{C*}_{(l'm')} W^*_{(l'm')}(\theta,0)\right] \Big\rangle \\ &= \sum_l \sqrt{\frac{2l+1}{8\pi}} N_l \left[iC^{GG}_l (X^*_{l,2} + X^*_{l,-2}) + C^{CC}_l (W^*_{l,2} - W^*_{l,-2})\right] \end{aligned} \tag{44}$$

The cross-correlation vanishes, $C^{UQ} = 0$, if parity is conserved in the early universe [2].

4 The Boltzmann Equation

The polarization distribution function of photons can be represented by the column vector $\mathbf{f} = (I_x, I_y, U)$ where the components are related to the Stokes parameters, $I = I_x + I_y$ and $Q = I_x - I_y$ [1]. After Fourier transforming the time dependence in the electromagnetic waves, $\mathbf{f}(\eta, x^i, \nu, \mu, \phi)$ is a function of conformal time η, position x^i, frequency of the electromagnetic radiation ν and the direction of photon propagation, μ and ϕ.

The time evolution of the distribution function is given by the Boltzmann equation

$$\frac{\partial \mathbf{f}}{\partial \eta} + \hat{n}^i \frac{\partial \mathbf{f}}{\partial x^i} = -\frac{d\nu}{d\eta}\frac{\partial \mathbf{f}}{\partial \nu} - q\,(\mathbf{f} - \mathbf{J})\,. \tag{45}$$

$q(\eta) = \sigma_T n_e a$ is the differential optical depth and has the meaning of scattering rate, $a(\eta)$ is the scale factor, σ_T is the Thomson cross-section, $n_e(\eta)$ is the number density of free electrons.

$$\mathbf{J}(\eta, x^i, \nu, \mu, \phi) = \frac{1}{4\pi}\int_{-1}^{1} d\mu' \int_0^{2\pi} d\phi' P(\mu, \phi, \mu', \phi')\mathbf{f}(\eta, x^i, \nu, \mu', \phi'), \tag{46}$$

where $\mu = \cos\theta$ and

$$P = \frac{3}{4}\begin{pmatrix} \mu^2\mu'^2\cos 2(\phi'-\phi) & -\mu^2\cos 2(\phi'-\phi) & \mu^2\mu'\sin 2(\phi'-\phi) \\ -\mu'^2\cos 2(\phi'-\phi) & \cos 2(\phi'-\phi) & -\mu'\sin 2(\phi'-\phi) \\ -2\mu\mu'^2\sin 2(\phi'-\phi) & 2\mu\sin 2(\phi'-\phi) & 2\mu\mu'\cos 2(\phi'-\phi) \end{pmatrix} \tag{47}$$

is the scattering matrix [1]. Primed index refer to incident and unprimed to scattered radiation. The term $-q\,(\mathbf{f} - \mathbf{J})$ is the effect of the Thomson scattering. The first part, $-q\mathbf{f}$, dampens the polarization and the second part, $q\mathbf{J}$, changes the polarization. The term $-\frac{d\nu}{d\eta}\frac{\partial \mathbf{f}}{\partial \nu}$ describes the change due to metric perturbations caused by the RGWs through the Sachs-Wolfe effect (A.3)

$$\frac{1}{\nu}\frac{d\nu}{d\eta} = \frac{1}{2}\frac{\partial h_{ij}}{\partial \eta}\hat{n}^i\hat{n}^j. \tag{48}$$

The perturbations caused by a gravitational wave propagating in the z-direction is, by eq. 18 and 19,

$$\begin{aligned} \frac{1}{2}\frac{\partial h_{ij}}{\partial \eta}\hat{n}^i\hat{n}^j &= \frac{1}{2}\frac{\partial}{\partial \eta}\left(h^+\epsilon^+_{ij} + h^\times\epsilon^\times_{ij}\right)\hat{n}_i\hat{n}_j \\ &= \frac{1}{2}\dot{h}^+(\eta)(1-\mu^2)\cos 2\phi + \frac{1}{2}\dot{h}^\times(\eta)(1-\mu^2)\sin 2\phi. \end{aligned} \tag{49}$$

Taking the statistical properties and the magnitudes to be the same for both the h^+ and the $h^\times$ waves, i.e. they have the same expectation values, they can be replaced by $h(\eta)$. The perturbed radiation is, for the + polarization

$$\frac{1}{\nu}\frac{d\nu}{d\eta} = -\frac{1}{2}(1-\mu^2)\cos(2\phi)\frac{d}{d\eta}h(\eta) \tag{50}$$

and for the cross polarization

$$\frac{1}{\nu}\frac{d\nu}{d\eta} = -\frac{1}{2}(1-\mu^2)\sin(2\phi)\frac{d}{d\eta}h(\eta). \tag{51}$$

The gravitational wave causes an angular intensity pattern. However the radiation is still unpolarized, consisting of an unperturbed part and a perturbed part, $\mathbf{a}^+(\mu,\phi)$ and $\mathbf{a}^\times(\mu,\phi)$ for respective polarization,

$$\mathbf{a}^{+}(\mu,\phi) = \frac{1}{2}(1-\mu^2)\cos 2\phi \begin{pmatrix} 1 \\ 1 \\ 0 \end{pmatrix}. \tag{52}$$

and

$$\mathbf{a}^{\times}(\mu,\phi) = \frac{1}{2}(1-\mu^2)\sin 2\phi \begin{pmatrix} 1 \\ 1 \\ 0 \end{pmatrix}. \tag{53}$$

As the perturbed radiation is Thomson scattered the distribution is changed and the scattering matrix introduces a perturbed, polarized, part $\mathbf{b}$ (A.2). For the + polarization

$$\mathbf{b}^{+}(\mu,\phi) = \frac{1}{2}\begin{pmatrix} (1+\mu^2)\cos 2\phi \\ -(1+\mu^2)\cos 2\phi \\ 4\mu\sin 2\phi \end{pmatrix} \tag{54}$$

and for the $\times$ polarization

$$\mathbf{b}^{\times}(\mu,\phi) = \frac{1}{2}\begin{pmatrix} (1+\mu^2)\sin 2\phi \\ -(1+\mu^2)\sin 2\phi \\ 4\mu\cos 2\phi \end{pmatrix}. \tag{55}$$

$(\mathbf{a},\mathbf{b})$ form a closed basis under Thomson scattering (A.4), and the perturbed part of the distribution function can therefore be generally described by a linear combination of these. Hence it is possible to divide $\mathbf{f}$ into one unperturbed part, $\mathbf{f}_0(\nu)$ and one perturbed part $\mathbf{f}_1(\eta, x^i, \nu, \mu, \phi)$,

$$\mathbf{f} = f_0\left[\begin{pmatrix} 1 \\ 1 \\ 0 \end{pmatrix} + \mathbf{f}_1\right] \tag{56}$$

where f_0 is the blackbody radiation,

$$f_0(\nu) = \frac{1}{e^{h\nu/kT}-1}. \tag{57}$$

$\mathbf{f}_1$ depend on what type of polarization the gravitational wave causing the perturbation have. To first order in the perturbations $\mathbf{f}_1$ for the + polarization

$$\begin{aligned} \mathbf{f}_1^{+} &= \frac{\zeta}{2}(1-\mu^2)\cos 2\phi \begin{pmatrix} 1 \\ 1 \\ 0 \end{pmatrix} + \frac{\beta}{2}\begin{pmatrix} (1+\mu^2)\cos 2\phi \\ -(1+\mu^2)\cos 2\phi \\ 4\mu\sin 2\phi \end{pmatrix} \\ &= \zeta(\eta, x^i, \nu, \mu)\mathbf{a}^{+} + \beta(\eta, x^i, \nu, \mu)\mathbf{b}^{+} \end{aligned} \tag{58}$$

and for the $\times$ polarization

$$\begin{aligned} \mathbf{f}_1^{\times} &= \frac{\zeta}{2}(1-\mu^2)\sin 2\phi \begin{pmatrix} 1 \\ 1 \\ 0 \end{pmatrix} + \frac{\beta}{2}\begin{pmatrix} (1+\mu^2)\sin 2\phi \\ -(1+\mu^2)\sin 2\phi \\ 4\mu\cos 2\phi \end{pmatrix} \\ &= \zeta(\eta, x^i, \nu, \mu)\mathbf{a}^{\times} + \beta(\eta, x^i, \nu, \mu)\mathbf{b}^{\times}. \end{aligned} \tag{59}$$

The explicit ϕ dependence is due to the angular dependence of the gravitational waves and the explicit μ dependence is simply chosen to simplify the evolution equations [9].

$\zeta \propto I_x + I_y = I$ represent the anisotropy of the photon distribution and $\beta \propto I_x - I_y = Q$ represent the polarization of photons [1].

If unpolarized radiation $\mathbf{f}_0$ enters the Boltzmann equation the different terms will be zero (A.4). Thus the time evolution of $\mathbf{f}$ is determined by the perturbed part, $f_0\mathbf{f}_1$, and eq. 45 is

$$f_0 \frac{\partial \mathbf{f}_1}{\partial \eta} + f_0 \hat{n}^i \frac{\partial \mathbf{f}_1}{\partial x^i} = -\frac{1}{f_0}\frac{d\nu}{d\eta}\frac{\partial \mathbf{f}}{\partial \nu} - f_0 q\left(\mathbf{f}_1 - \mathbf{J}(\mathbf{f}_1)\right). \tag{60}$$

Since $\frac{d\nu}{d\eta}$, eq. 50 and 51, is of first order in the perturbations, $\frac{\partial \mathbf{f}}{\partial \nu}$ can, in the first order approximation be replaced with $\frac{\partial \mathbf{f}_0}{\partial \nu_0}$. ν_0 is the unperturbed frequency. The anisotropy and polarization thus have the same frequency dependence and since neither q nor P depend on ν, the different frequencies can be treated independently. Dividing by f_0 to obtain

$$\frac{\partial \mathbf{f}_1}{\partial \eta} + \hat{n}^i \frac{\partial \mathbf{f}_1}{\partial x^i} = -\frac{1}{2}\frac{\nu_0}{f_0}\frac{\partial f_0}{\partial \nu_0}\frac{\partial h_{ij}}{\partial \eta}\hat{n}^i\hat{n}^j - q\left(\mathbf{f}_1 - \mathbf{J}\right). \tag{61}$$

Taking the spatial Fourier transformation gives

$$\frac{\partial \tilde{\mathbf{f}}_1}{\partial \eta} + i\hat{n}^i k_i \tilde{\mathbf{f}}_1 = -\frac{1}{2}\frac{\nu_0}{f_0}\frac{\partial f_0}{\partial \nu_0}\frac{\partial h_{ij}}{\partial \eta}\hat{n}^i\hat{n}^j - q(\eta)\left[\tilde{\mathbf{f}}_1 - \tilde{\mathbf{J}}\right] \tag{62}$$

For the gravitational wave travelling in the z direction, i.e. $\hat{z} = \hat{k}$, $\frac{\hat{n}^i k_i}{k} = \mu$ and the angle of $\hat{n}^i$ in the plane perpendicular to the vector $\hat{k}$ is $\phi_k = \phi$. After some calculations (A.4) the anisotropy and polarization can be described by two coupled differential equations,

$$\dot{\xi}_k + (ik\mu + q)\,\xi_k(\eta,\mu) = \dot{h}_k(\eta) \tag{63}$$

and

$$\dot{\beta}_k + (ik\mu + q)\,\beta_k(\eta,\mu) = \frac{3}{16}q\int_{-1}^{1} d\mu' \left[(1+\mu'^2)^2\beta_k(\eta,\mu') - \frac{1}{2}(1-\mu'^2)^2\xi_k(\eta,\mu')\right], \tag{64}$$

where $\xi_k = \zeta_k + \beta_k$. The subscript k is the Fourier mode of the gravitational waves.

5 Power Spectra and Correlation Functions

5.1 Expanding the Solutions

Eq. 63 and 64 have not been solved but once once the solution is found it can be expanded in Legendre functions,

$$\xi(\eta,\mu) = \sum_l (2l+1)\xi_l(\eta)P_l(\mu) \tag{65}$$

and

$$\beta(\eta,\mu) = \sum_l (2l+1)\beta_l(\eta)P_l(\mu). \tag{66}$$

The expansion coefficients are

$$\xi_l(\eta) = \frac{1}{2}\int_{-1}^{1} d\mu \xi(\eta,\mu)P_l(\mu) \tag{67}$$

and

$$\beta_l(\eta) = \frac{1}{2}\int_{-1}^{1} d\mu \beta(\eta,\mu)P_l(\mu) \tag{68}$$

The coefficients, $a^G_{(lm)}$ and $a^C_{(lm)}$, from the expansion of the polarization tensor P_{ab}, eq. 33, determining the electric and magnetic polarization spectra can then be described as a function of ξ_l and β_l. After some algebra, eq. 34 and 35, is (A.6)

$$\begin{aligned} a^G_{(lm)} &= \frac{1}{8}(\delta_{m,2}+\delta_{m,-2})\sqrt{2\pi(2l+1)}\left[\frac{(l+2)(l+1)\beta_{l-2}}{(2l-1)(2l+1)}\right. \\ &\left. +\frac{6(l-1)(l+2)\beta_l}{(2l+3)(2l-1)} + \frac{l(l-1)\beta_{l+2}}{(2l+3)(2l+1)}\right] \end{aligned} \tag{69}$$

and

$$a^C_{(lm)} = \frac{-i}{4}\sqrt{\frac{2\pi}{(2l+1)}}(\delta_{m,2}-\delta_{m,-2})\left[(l+2)\beta_{l-1}+(l-1)\beta_{l+1}\right]. \tag{70}$$

5.2 Polarization Power Spectra

The polarization power spectra, eq. 36, is determined by, $a^G_{(lm)}$ and $a^C_{(lm)}$. Calculating the power spectra, the subscript k from the different Fourier modes as well as the two different types of gravitational waves , h^+ and $h^\times$, have to be remembered. The linearity enables a summation over all k and the two gravitational wave polarizations to get the total polarization caused by relic gravitational waves. For one wave the polarization is

$$C^{GG}_l(k) = \frac{1}{(2l+1)}\sum_m |a^G_{(lm)}(k)|^2 \tag{71}$$

$$C^{CC}_l(k) = \frac{1}{(2l+1)}\sum_m |a^C_{(lm)}(k)|^2. \tag{72}$$

Taking all Fourier modes and both types of RGWs into account,

$$\begin{aligned} C^{GG}_l &= \frac{2}{(2\pi)^3(2l+1)}\int\sum_m |a^G_{(lm)}(k)|^2 d^3k \\ &= \frac{1}{\pi^2(2l+1)}\int\sum_m |a^G_{(lm)}(k)|^2 k^2 dk \end{aligned}$$

$$= \frac{1}{16\pi}\int\left|\frac{(l+2)(l+1)\beta_{l-2}}{(2l-1)(2l+1)}+\frac{6(l-1)(l+2)\beta_l}{(2l+3)(2l-1)} +\frac{l(l-1)\beta_{l+2}}{(2l+3)(2l+1)}\right|^2 k^2dk \tag{73}$$

$$C_l^{CC} = \frac{1}{\pi^2(2l+1)}\int\sum_m |a^C_{(lm)}(k)|^2k^2dk = \frac{1}{4\pi}\int\left|\frac{(l+2)\beta_{l-1}}{2l+1}+\frac{(l-1)\beta_{l+1}}{2l+1}\right|k^2dk \tag{74}$$

The cross-correlation power spectrum vanishes, if parity is conserved in the early universe,

$$C_l^{GC} = \sum_m \frac{a^{G*}_{(lm)}a^C_{(lm)}}{(2l+1)} \propto (\delta_{m,2}+\delta_{m,-2})(\delta_{m,2}-\delta_{m,-2}) = 0. \tag{75}$$

6 Time Evolution of RGWs

The time evolution of Relic Gravitational Waves, $\dot{h}$, is the source of the CMB polarization, eq. 63. Einstein's field equations in the Friedmann-Lemaître-Robertson-Walker-universe leads to the equation of motion for a RGW of mode k,

$$\ddot{h} + 2\frac{\dot{a}}{a}\dot{h} + k^2h = 0. \tag{76}$$

The initial values are

$$h(\eta = 0) = h(k) \tag{77}$$

$$\dot{h}(\eta = 0) = 0 \tag{78}$$

with

$$\frac{k^3}{2\pi^2}|h(k)|^2 = P_h(k) = A_T\left(\frac{k}{k_0}\right)^{n_T} \tag{79}$$

where P_h is the primordial power spectrum of RGW, A_T the amplitude, n_T is the tensor spectrum index and $k_0 = 0.005(Mpc)^{-1}$ is the pivot wavenumber. The effect of the free streaming neutrinos has been ignored and could lower the peaks of the spectrum slightly.

The scale factor $a(\eta)$ can be determined by the Friedmann equation

$$\dot{a}^2 = H_0^2[\Omega_r + a\Omega_m + a^4\Omega_\Lambda] \tag{80}$$

where $H_0 = 0.72$ is the Hubble parameter at present time and Ω_r, Ω_m, Ω_Λ are densities of radiation, matter and dark energy. [1]

However, the analytical derivations will have to rely on an approximation of $a(\eta)$ by a sudden transition between consecutive stages (A.8).

The redshift can be expressed as a function of the scale factor

$$1 + z_\eta = \frac{\lambda_0}{\lambda_\eta} = \frac{a_0}{a_\eta} = \frac{1}{a_\eta}. \tag{81}$$

At the transition between a radiation and a matter dominated universe, the two corresponding terms in eq. 80 is equal,

$$\Omega_r = a\Omega_m \Rightarrow a_e = \frac{\Omega_r}{\Omega_m}. \tag{82}$$

Setting the fractional densities to be $\Omega_r = 8.39 \times 10^{-5}$, $\Omega_m = 0.27$ and $\Omega_\Lambda = 0.73$, matter/radiation equality takes place at redshift $z_e = 3229$, i.e. $\eta_e/\eta_0 = 0.009$, while matter/dark-energy equality is found at $z = 0.39$, i.e. $\eta_E/\eta_0 = 0.875$. Setting the redshift of decoupling to $z_d = 1088$ [11], gives the conformal time of decoupling $\eta_d/\eta_0 = 0.0224$.

Solving eq. 76 in this approximation (A.7) gives

$$h(\eta) = A_0 j_0(k\eta), \qquad (\eta \leq \eta_e), \tag{83}$$

$$h(\eta) = A_0 \frac{\eta_e}{\eta}(A_1 j_1(k\eta) + A_2 y_1(k\eta)), \qquad (\eta_e < \eta \leq \eta_E), \tag{84}$$

with coefficients

$$A_0 = \left(\frac{2\pi^2 A_T}{k^3}\left(\frac{k}{k_0}\right)^{n_T}\right)^{1/2}, \tag{85}$$

$$A_1 = \frac{3k\eta_e - k\eta_e\cos(2k\eta_e) + 2\sin(2k\eta_e)}{2k^2\eta_e^2} \tag{86}$$

and

$$A_2 = \frac{2 - 2k^2\eta_e^2 - 2\cos(2k\eta_e) - k\eta_e\sin(2k\eta_e)}{2k^2\eta_e^2}. \tag{87}$$

Taking the time derivative of the gravitational wave $\dot{h}(\eta)$ and using the relation for spherical Bessel and Neumann functions [6],

$$\frac{d}{dx}\left(x^{-n} f_n(x)\right) = -x^{-n} j_{n+1}(x). \tag{88}$$

The time evolution, $\dot{h}(\eta)$, of a gravitational wave is

$$\begin{aligned} \dot{h}(\eta) &= -A_0\frac{\eta_e}{\eta}k\left(A_1\left(\frac{j_1(k\eta)}{k\eta} + j_1'(k\eta)\right) + A_2\left(\frac{y_1(k\eta)}{k\eta} + y_1'(k\eta)\right)\right) \\ &= -A_0\frac{\eta_e}{\eta}k\left(A_1 j_2(k\eta) + A_2 y_2(k\eta)\right), \end{aligned} \tag{89}$$

during the matter dominated era. For the radiation dominated universe

$$\dot{h}(\eta) = A_0 k\dot{j}(k\eta) = -A_0 k j_1(k\eta). \tag{90}$$

The evolution of the RGWs are important primarily in the vicinity of the decoupling η_d, when the polarization is generated. The degree of polarization caused by the gravitational wave around $\eta = \eta_d$ depends on the wavenumber k. The dependence of $h(\eta_d)$ and $\dot{h}(\eta_d)$ on k are shown in fig. 2 and fig. 3 respectively.

Before the RGW enter the horizon, the different parts of the wave have never been in contact and it is left relatively intact, i.e. the amplitude stays the same, as the universe expand. As the wave enters the horizon it quickly decreases before entering a slowly decaying oscillatory state. Fig. 4 contains gravitational waves for three different wavenumbers k and the steep slope of the wave with $k = 1000$ occur at conformal time $\eta \simeq 0.001$, i.e. when the wavelength equals the horizon size.

The exact solution of eq. 80 in the radiation and matter dominated eras is,

$$a(\tau) = a_e \tau(\tau + 2) \tag{91}$$

where $\tau = (\sqrt{2} - 1)\eta/\eta_e$. The transition between the two stages is smooth, in the new parameter, the time evolution is given by

$$h'' + 2\frac{a'}{a}h' + k^2 h = 0 \tag{92}$$

where prime denotes $\frac{d}{d\tau}$. To improve the sudden transition approximation one can use the Wentzel-Kramers-Brillouin approximation [16], to solve this equation. [1]

However the WKB approximation will not be used in any analytic calculations throughout this thesis but is used to obtain numerical solutions to eq. 92 shown in fig. 2 and 3. Fig. 2 and 3 also contains numerical solutions of eq. 76. This has been done with $a(\eta)$ calculated numerically from eq. 80 taking the fractional densities $\Omega_r = 8.36 \times 10^{-5}$, $\Omega_b = 0.044$, $\Omega_{dm} = 0.225$ and $\Omega_\Lambda = 0.73$ [1].

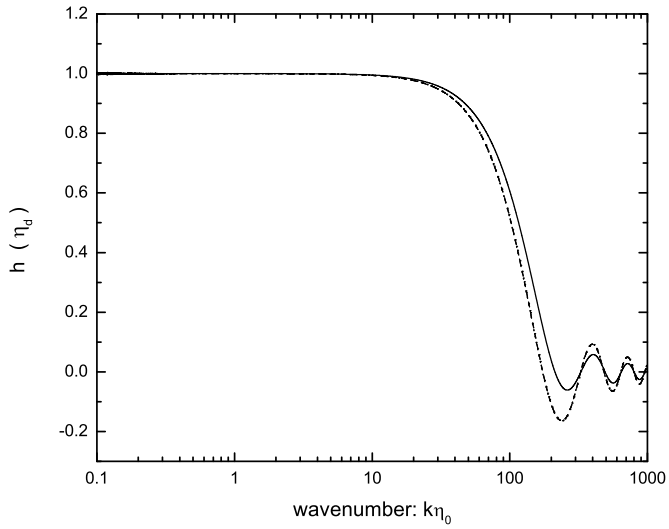

Fig. 2: A RGW at decoupling, $h(\eta_d)$, depending on wavenumber k. The sudden transition approximation (solid line), WKB approximation (dashed line) and numerical calculations (dotted line). The numerical and WKB lines are nearly identical and are hard to distinguish by the naked eye. The initial amplitude is set to $h(k) = 1$. Figure from [1].

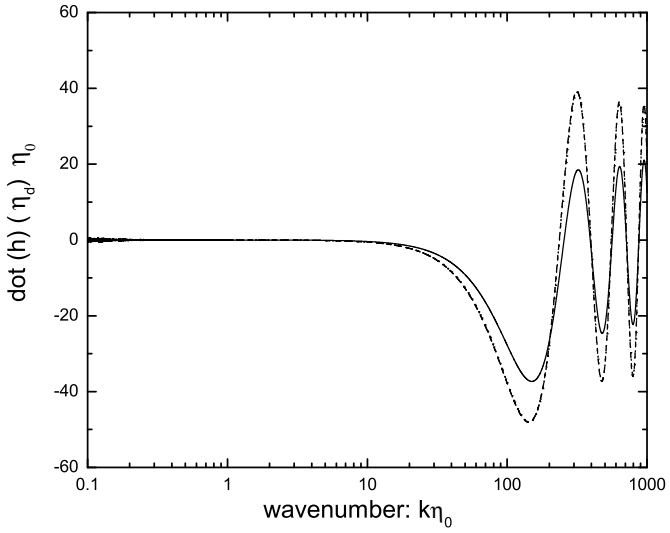

Fig. 3: Time derivative of the RGW, $\dot{h}(\eta_d)$, depending on wavenumber k. The sudden transition approximation (solid line), WKB approximation (dashed line) and numerical calculations (dotted line). The numerical and WKB lines are nearly identical. The initial amplitude is set to $h(k) = 1$. Figure from [1].

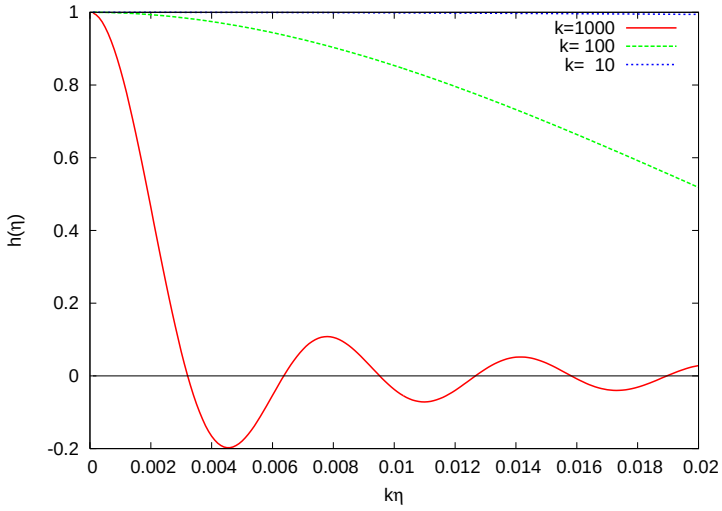

Fig. 4: RGW of three different Fourier modes, $k = 1000,\ 100,\ 10$, depending on the conformal time η. The $k = 1000$ wave enters the horizon at $k\eta = 0.001$ and the steep slope demonstrates the quick decrease of amplitude of a RGW as it enters the horizon.

7 Visibility Function

In the early universe when baryons were ionized and tightly coupled with the photons through Thomson scattering, photons were repeatedly scattered causing a bath of unpolarized radiation. When the temperature decreased the electrons and ions formed neutral atoms, decoupling the photons and baryons. It was at the time of decoupling that the last scattering took place and the probability that a photon was last scattered at time η is described by the visibility function,

$$V(\eta) = q(\eta)e^{-\kappa(\eta_0,\eta)}. \tag{93}$$

The visibility function comes from solving the ionization equations during the recombination [1]. The differential optical depth $q = \sigma_T n_e(\eta)a(\eta)$ depends on the number density of free electrons n_e. The optical depth

$$\kappa(\eta_0, \eta) = \int_{\eta}^{\eta_0} q(\eta)d\eta \tag{94}$$

describes the photon transparency of the universe. As electrons and ions form atoms the number density of free electrons n_e rapidly fall off towards zero. Thus both q and κ quickly approach zero during the decoupling and thereby $V(\eta) \simeq 0$ for $\eta > \eta_d$. Going backwards in time, before η_d, the number density of free electrons increase as the universe grows smaller and both q and $\kappa(\eta)$ increase. The visibility function is then dominated by the exponential which cause $V(\eta)$ to approach zero. Since the visibility function is a probability distribution, it has to be normalized to one,

$$\int_0^{\eta_0} V(\eta)d\eta = 1. \tag{95}$$

The visibility function is often approximated by a Gaussian function [9]

$$V(\eta) = V(\eta_d)e^{\left(-\frac{(\eta-\eta_d)^2}{2\Delta\eta_d^2}\right)} \tag{96}$$

fitted to numerical calculations. $V(\eta_d)$ is the amplitude at, and $\Delta\eta_d$ is the width of, decoupling. WMAP data give $\Delta\eta_d/\eta_0 = 0.00143$ [1]. Following [1] a half-Gaussian fitting consisting of two half-Gaussian functions is used in order to improve the approximation.

$$V(\eta) = \begin{cases} V(\eta_d)e^{-\frac{(\eta-\eta_d)^2}{2\Delta\eta_{d1}^2}} & \eta \leq \eta_d \\ V(\eta_d)e^{-\frac{(\eta-\eta_d)^2}{2\Delta\eta_{d2}^2}} & \eta > \eta_d \end{cases} \tag{97}$$

with $(\Delta\eta_{d1} + \Delta\eta_{d2})/2 = \Delta\eta_d$, $\Delta\eta_{d1}/\eta_0 = 0.00110$ and $\Delta\eta_{d2} = 0.00176$. Both approximations obey eq. 95. The two approximations are plotted together with the optical depth $\kappa(\eta)$ and the differential optical depth $q(\eta)$ in fig. 5. A comparison with numerical calculations of the visibility function is found in fig. 6.

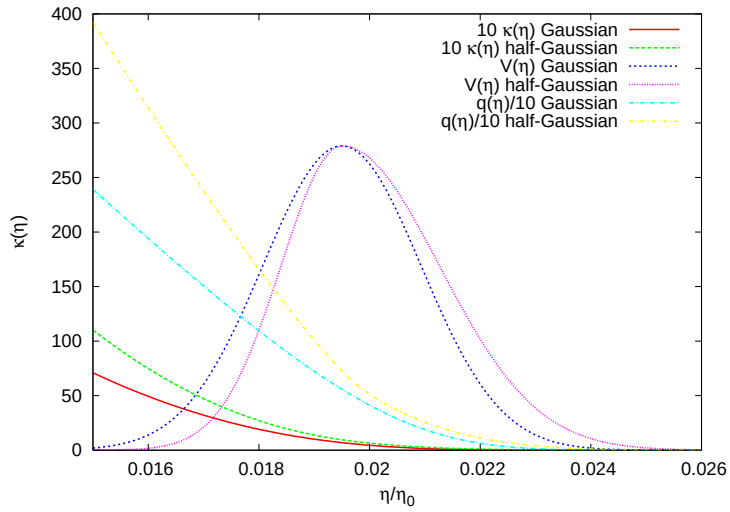

Fig. 5: The visibility function $V(\eta)$, optical depth $\kappa(\eta) \times 10$ and differential optical depth $q(\eta)/10$ during decoupling. The latter two have been rescaled for graphical demonstration.

Neither the Gaussian nor the half-Gaussian approximation manages to resemble the steep uphill slope and the long tail very well, but the half-Gaussian does a significantly better job. The effects of the approximation will be discussed in more detail in later sections.

8 Solving the Boltzmann Equation

To get the polarization power spectra, eq. 73 and 74, the differential equations for ξ_k eq. 63 and β_k eq. 64 have to be solved. The subscript, k of ξ, β and $\dot{h}$, will be hidden in this section for notational simplicity.

$$\dot{\xi} + (ik\mu + q)\,\xi(\eta,\mu) = \dot{h} \tag{98}$$

$$\dot{\beta} + (ik\mu + q)\,\beta(\eta,\mu) = \frac{3}{16} q \int_{-1}^{1} d\mu' \left[(1+\mu'^2)^2 \beta(\mu') - \frac{1}{2}(1-\mu'^2)^2 \xi(\mu') \right] \tag{99}$$

Initially the radiation is unperturbed, i.e. $\xi(\eta = 0) = 0$, and the solution to eq. 98 is

$$\begin{aligned} \xi(\eta) &= \int_0^\eta \dot{h}(\eta') e^{-\int_{\eta'}^{\eta} (ik\mu+q) d\eta''} d\eta' \\ &= \int_0^\eta \dot{h}(\eta') e^{-\kappa(\eta,\eta')} e^{ik\mu(\eta'-\eta)} d\eta'. \end{aligned} \tag{100}$$

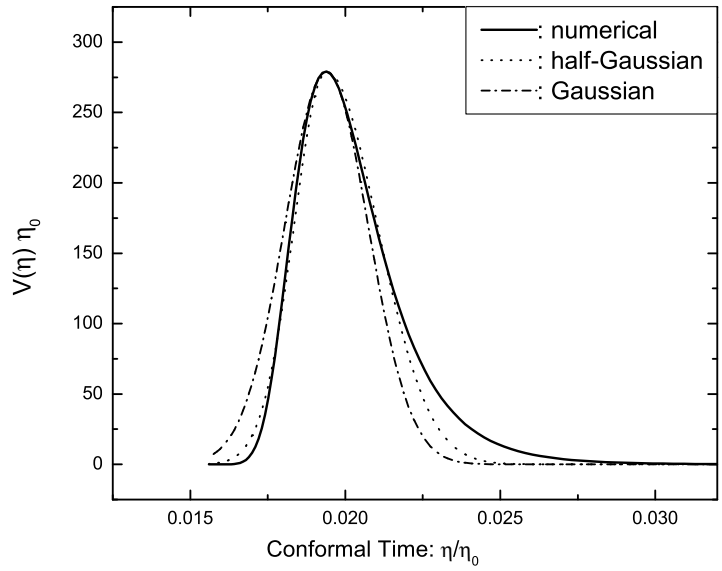

Fig. 6: The visibility function $V(\eta)$ as a function of conformal time η. Numerical results (solid line), half-Gaussian approximation (dots) and Gaussian approximation (dash). $\eta_d/\eta_0 = 0.0195$, number from [1] which does not seem to agree with solving the equations, and the three curves are normalized $\int V d\eta = 1$. Figure from [1].

Expanding ξ and β in Legendre polynomials according to eq. 65 and eq. 66, the right side of eq. 99 is

$$\begin{aligned} G(\eta) &= \int_{-1}^{1} d\mu' \left[(1+\mu'^2)^2 \beta(\eta,\mu') - \frac{1}{2}(1-\mu'^2)^2 \xi(\eta,\mu') \right] \\ &= \frac{3}{16} \sum_l (2l+1) \int_{-1}^{1} d\mu' (1+\mu'^2)^2 \beta_l P_l + \\ &\quad \frac{3}{16} \sum_l (2l+1) \int_{-1}^{1} d\mu' (1-\mu'^2)^2 \xi_l P_l \\ &= \frac{3}{16} \sum_l (2l+1) \int_{-1}^{1} d\mu' \left(\frac{196}{105} P_0 + \frac{200}{105} P_2 + \frac{8}{35} P_4 \right) \beta_l P_l \\ &\quad + \frac{3}{16} \sum_l (2l+1) \int_{-1}^{1} d\mu' \left(\frac{56}{105} P_0 - \frac{80}{105} P_2 + \frac{8}{35} P_4 \right) \xi_l P_l. \quad (101) \end{aligned}$$

The integral is evaluated, by using the orthogonality relation for Legendre polynomials

$$\int_{-1}^{1} d\mu' P_l(\mu') P_{l'}(\mu') = \frac{2}{2l+1}\delta_{ll'} \text{ [6]}, \tag{102}$$

with the result

$$G(\eta) = \frac{3}{35}\beta_4 + \frac{5}{7}\beta_2 + \frac{7}{10}\beta_0 - \frac{3}{70}\xi_4 + \frac{1}{7}\xi_2 - \frac{1}{10}\xi_0. \tag{103}$$

Eq. 99 is then

$$\dot{\beta} + [ik\mu + q]\beta = qG, \tag{104}$$

with the solution, $\beta(\eta = 0) = 0$,

$$\beta(\eta, \mu) = \int_0^{\eta} G(\eta') q(\eta') e^{-\kappa(\eta,\eta') + ik\mu(\eta' - \eta)} d\eta'. \tag{105}$$

Setting the above limit to the present time, η_0, and identifying the visibility function, from eq. 93, resulting in

$$\beta(\eta_0, \mu) = \int_0^{\eta_0} G(\eta) V(\eta) e^{ik\mu(\eta - \eta_0)} d\eta. \tag{106}$$

The integral contains the unknown functions β_l and ξ_l. Take the expansion, eq. 65, and put it into eq. 98,

$$\sum_l (2l+1)\dot{\xi}_l P_l = -q \sum_l (2l+1)\xi_l P_l - ik \sum_l \xi_l (2l+1)\mu P_l + P_0(\mu)\dot{h}. \tag{107}$$

Use the recurrence relation for the Legendre polynomials [6],

$$(2l+1)\mu P_l = (l+1)P_{l+1} + lP_{l-1}. \tag{108}$$

The last sum in eq. 107 can be expressed as

$$\sum_l \xi_l (2l+1)\mu P_l = \sum_{l'=l+1} \xi_{l'-1} l' P'_l + \sum_{l''=l-1} \xi_{l''+1}(l''+1)P_{l''}. \tag{109}$$

Because of the orthogonality of P_l the relation has to be true for every l, thus after renaming the dummy indices a system of coupled differential equations for $\xi(\eta)$ is obtained. Repeating the procedure for β and the result is

$$\dot{\xi}_0 = -q\xi_0 - ik\xi_1 + \dot{h} \tag{110}$$

$$\dot{\beta}_0 = -\frac{3}{10}q\beta_0 - ik\beta_1 + q\left(\frac{3}{35}\beta_4 + \frac{5}{7}\beta_2 - \frac{3}{70}\xi_4 - \frac{1}{7}\xi_2 - \frac{1}{10}\xi_0\right) \tag{111}$$

$$\dot{\xi}_l = -q\xi_l - \frac{ik}{2l+1}\left[l\xi_{l-1} + (l+1)\xi_{l+1}\right],\ l \geq 1 \tag{112}$$

$$\dot{\beta}_l = -q\beta_l - \frac{ik}{2l+1}\left[l\beta_{l-1} + (l+1)\beta_{l+1}\right],\ l \geq 1. \tag{113}$$

$1/q$ is the mean free path of photons. In the tight coupling limit the mean free path is close to zero and q tends to infinty. Expanding to first order in the small parameter $1/q$, starting with unperturbed radiation, the equations reduce to (A.9)

$$\dot{\xi}_0 + q\xi_0 = \dot{h} \tag{114}$$

$$\dot{\beta}_0 + \frac{3}{10}q\beta_0 = -\frac{1}{10}q\xi_0 \tag{115}$$

$$\xi_l = \beta_l = 0,\ l \geq 1. \tag{116}$$

$G(\eta)$ from eq. 103 is then

$$G(\eta) = \frac{1}{10}(7\beta_0 - \xi_0). \tag{117}$$

and satisfies

$$\dot{G} + \frac{3}{10}qG = -\frac{1}{10}\dot{h}, \tag{118}$$

with the solution

$$G(\eta) = -\frac{1}{10}\int_0^\eta \dot{h}(\eta')e^{-(3/10)\kappa(\eta,\eta')}d\eta'. \tag{119}$$

Substituting this into eq. 106 for $\beta(\eta_0)$ yields

$$\begin{aligned}\beta(\eta_0,\mu) &= \int_0^{\eta_0} V(\eta)\left[-\frac{1}{10}\int_0^\eta \dot{h}(\eta')e^{-(3/10)\kappa(\eta,\eta')}d\eta'\right]e^{ik\mu(\eta-\eta_0)}d\eta \\ &= -\frac{1}{10}\int_0^{\eta_0} d\eta V(\eta)e^{ik\mu(\eta-\eta_0)}\int_0^\eta d\eta'\dot{h}(\eta')e^{-(3/10)\kappa(\eta')+(3/10)\kappa(\eta)}\end{aligned} \tag{120}$$

where $\kappa(\eta,\eta') = \kappa(\eta') - \kappa(\eta)$ and $\kappa(\eta) = \kappa(\eta_0,\eta)$. The tight coupling approximation is only good on scales larger than the mean free path of photons. On smaller scales the anisotropies and polarizations will be damped by photon diffusion, to include this effect the second order of $1/q$ is needed [1]. Meaning that ξ_1 differs from zero because of the ξ_0 source term in the differential equation. The equations for ξ in this second order approximation of the tight coupling is (A.9)

$$\dot{\xi}_0 = -q\xi_0 - ik\xi_1 + \dot{h}, \tag{121}$$

$$\dot{\xi}_1 = -q\xi_1 - \frac{ik}{3}\xi_0, \tag{122}$$

$$\xi_l = 0,\ l \geq 2. \tag{123}$$

According to [1] this leads to an additional damping term $\exp\left(-\int q d\eta\right)$. However, this factor is present in the first order approximation as well. See appendix (B) for further discussion. This section will be completed as if the factor occured.

Keeping the tight-coupling limit for the polarization β, β_0 also gets the damping factor

$$\dot{\beta}_0 = -\frac{3q}{10}\beta_0 - \frac{q}{10}\xi_0. \tag{124}$$

The extra factor appear in eq. 118 and the solution for the polarization inherits it through the solution of $G(\eta)$. Eq. 120 takes the form

$$\beta(\eta_0,\mu) = -\frac{1}{10}\int_0^{\eta_0} d\eta V(\eta) e^{ik\mu(\eta-\eta_0)} \int_0^{\eta} d\eta' \dot{h}(\eta') e^{-(3/10)\kappa(\eta')-(7/10)\kappa(\eta)}. \tag{125}$$

Since $V(\eta)$ peaks around η_d while $\exp(-(3/10)\kappa(\eta''))\approx 0$ when $\eta<\eta_d$ and $\exp(-(3/10)\kappa(\eta''))\approx 1$ when $\eta>\eta_d$, $\dot{h}(\eta)$ can be taken outside the integrals approximating it with $\dot{h}(\eta_d)$. However, this approximation is only good at long wavelengths when $\dot{h}(\eta)$ varies slowly over $V(\eta)$. This can be improved by taking the average of $\dot{h}(\eta)$ over the visibility function,

$$\left\langle \dot{h}_d(\eta) \right\rangle = \int_0^{\eta_0} d\eta V(\eta)\dot{h}(\eta). \tag{126}$$

The resulting equation for the polarization is

$$\beta(\eta_0,\mu) = -\frac{1}{10}\int_0^{\eta_0} d\eta V(\eta) e^{ik\mu(\eta-\eta_0)}\dot{h}(\eta) \int_0^{\eta} d\eta' e^{-(3/10)\kappa(\eta')-(7/10)\kappa(\eta)}. \tag{127}$$

Define $x\equiv\kappa(\eta')/\kappa(\eta)$ and replace η'. Since $V(\eta)$ peaks around η_d with width $\Delta\eta_d$, $d\eta\approx\frac{dx}{x}\Delta\eta_d$ holds approximately.

$$\beta(\eta_0,\mu) = -\frac{1}{10}\Delta\eta_d \int_0^{\eta_0} d\eta' V(\eta') e^{ik\mu(\eta'-\eta_0)}\dot{h}(\eta) \int_1^{\infty} \frac{dx}{x} e^{-(3/10)\kappa(\eta)x-(7/10)\kappa(\eta)} \tag{128}$$

Comparing the Legendre expansion of β, eq. 68, and ξ, eq. 67, with

$$e^{ikr\mu} = \sum_{l=0}^{\infty}(2l+1)i^l j_l(kr)P_l(\mu) \tag{129}$$

and noting that the only dependence on μ in $\beta(\eta_0,\mu)$ is in the form of the exponential $\exp(ik\mu(\eta'-\eta))$ leads to

$$\begin{aligned}
\beta_l(\eta_0) &= \frac{1}{2}\int_{-1}^{1} d\mu\beta(\eta_0,\mu)P_l(\mu) \\
&= -\frac{1}{20}\int_0^{\eta_0} d\eta V(\eta)\sum_{l'=0}^{\infty} i^{l'} j_{l'}(k(\eta-\eta_0)P_{l'}(\mu)P_l(\mu)\dot{h}(\eta) \\
&\quad \int_1^{\infty}\frac{dx}{x}e^{-(3/10)\kappa(\eta')-(7/10)\kappa(\eta)} \\
&= -\frac{1}{10}\Delta\eta_d i^l \int_0^{\eta_0} d\eta V(\eta)\dot{h}(\eta) j_l(k(\eta-\eta_0)) \\
&\quad \int_1^{\infty}\frac{dx}{x}e^{-(3/10)\kappa(\eta)x-(7/10)\kappa(\eta)}.
\end{aligned} \tag{130}$$

The approximations of $V(\eta)$ contains a term of the type $e^{\gamma(\eta-\eta_d)^2}$ where γ is a constant, $\dot{h}$ contains a mixture of oscillating modes $e^{ik\eta}$ and $e^{-ik\eta}$ and so does the spherical Bessel functions. Therefore $\dot{h}(\eta)j(k(\eta-\eta_0))$ will contain terms proportional to $e^{-ibk(\eta-\eta_0)}$ with $b\in[-2,2]$. By using the formula [1]

$$\int_{-\infty}^{\infty} e^{-\gamma y^2}e^{ibky}dy = e^{-((bk)^2/4\gamma)}\int_{-\infty}^{\infty} e^{-\gamma y^2}dy, \tag{131}$$

with $y=k(\eta-\eta_d)$ and γ identified from the Gaussian or half-Gaussian approximation of the visibility function.

$$\begin{aligned}
&\int_0^{\eta_0} d\eta V(\eta)\dot{h}(\eta)j_l(k(\eta-\eta_0)) \simeq \int_0^{\eta_0} d\eta e^{\gamma(\eta-\eta_d)^2}e^{-ibk(\eta-\eta_0)}\\
&\approx \int_{-\infty}^{\infty} d\eta e^{\gamma(\eta-\eta_d)^2}e^{-ibk(\eta-\eta_0)} = e^{-((bk)^2/4\gamma)}\int_{-\infty}^{\infty} d\eta e^{-\gamma(\eta-\eta_d)^2}\\
&\simeq e^{-((bk)^2/4\gamma)}\dot{h}(\eta_d)j_l(k(\eta_d-\eta_o))\int_0^{\eta_0} d\eta V(\eta).
\end{aligned} \tag{132}$$

The Gaussian approximation give

$$e^{-((bk)^2/4\gamma)} = e^{-\alpha(k\Delta\eta_d)^2} \tag{133}$$

with $\alpha\in[0,2]$. The half Gaussian fitting will give two different terms. The integral will split into two and then merge when going back to the general expression again. The terms are

$$e^{-((bk)^2/4\gamma)} = \frac{1}{2}[e^{-\alpha(k\Delta\eta_{d1})^2}+e^{-\alpha(k\Delta\eta_{d2})^2}] \equiv D(k). \tag{134}$$

The remaining integral is

$$\int_0^{\eta_0} d\eta V(\eta)\int_1^{\infty}\frac{dx}{x}e^{-(3/10)\kappa(\eta)x}e^{-(7/10)\kappa(\eta)}. \tag{135}$$

Making the substitution

$$d\kappa = -q(\eta)d\eta \Rightarrow \frac{d\kappa}{q} = d\eta;\ V(\eta) = qe^{-\kappa(\eta)} \tag{136}$$

gives

$$\int_0^{\infty} d\kappa e^{-(17/10)\kappa}\int_1^{\infty}\frac{dx}{x}e^{-(3/10)\kappa x}. \tag{137}$$

Since $\kappa(\eta)\simeq 0$ when η is large and $\kappa(\eta)\to\infty$ when $\eta\to 0$

$$\int_0^{\infty} d\kappa e^{-(17/10)\kappa}\int_1^{\infty}\frac{dx}{x}e^{-(3/10)\kappa x}$$

$$= -\int_1^\infty \frac{dx}{x}\left[\left(\frac{17}{10}+\frac{3}{10}x\right)^{-1} e^{-(17/10)\kappa-(3/10)x\kappa}\right]_0^\infty$$
$$= 10\int_1^\infty \frac{dx}{x}\frac{1}{17+3x} = 10\int_1^\Lambda dx\left(\frac{1}{x}-\frac{3}{17+3x}\right)$$
$$= \frac{10}{17}\ln\left(\frac{20}{3+17/\Lambda}\right) = /\Lambda\to\infty/ = \frac{10}{17}\ln\frac{20}{3}. \quad (138)$$

Combining this with the results in eq. 132 gives the approximate solution for the polarization

$$\beta_l(\eta_0) = \frac{1}{17}\ln\frac{20}{3} i^l \Delta\eta_d \dot{h}(\eta_d) j_l(k(\eta_d-\eta_0))D(k) \quad (139)$$

where

$$D(k) = \frac{1}{2}\left(e^{-\alpha(k\Delta\eta_{d1})^2} + e^{-\alpha(k\Delta\eta_{d2})^2}\right). \quad (140)$$

If the Gaussian fitting had been used, $D(k)$ would have been

$$D(k) = e^{-\alpha(k\Delta\eta_d)^2} \quad (141)$$

Together with eq. 73 and eq. 74 the expression for the magnetic and electric polarization spectra is calculated,

$$C_l^{XX} = \frac{1}{16\pi}\left(\frac{1}{17}\ln\frac{20}{3}\right)^2 \int P_{Xl}^2(k(\eta-\eta_0))|\dot{h}(\eta_d)|^2\Delta\eta_d^2 D^2(k)k^2 dk. \quad (142)$$

The index X can be either G or C,

$$P_{Gl}(x) = \frac{(l+2)(l+1)}{(2l-1)(2l+1)}j_{l-2}(x) + \frac{6(l-1)(l+2)}{(2l-1)(2l+3)}j_l(x) + \frac{l(l-1)}{(2l+3)(2l+1)}j_{l+2}(x) \quad (143)$$

and

$$P_{Cl}(x) = \frac{2(l+2)}{2l+1}j_{l-1}(x) - \frac{2(l-1)}{2l+1}j_{l+1}(x). \quad (144)$$

9 Results and Discussion

The CMB polarization was generated by RGWs at the surface of last scattering, i.e. when matter and light decoupled. The greatest contribution to the polarization is from RGWs with wavelengths that entered the horizon just before the last scattering. This is because RGWs with wavelengths larger than the horizon size at decoupling does not change during the time the decoupling takes place. When a gravitational wave enters the horizon the amplitude quickly decreases and then enters an oscillatory stage with a slowly decaying amplitude [8]. Therefore the waves that enter the horizon at penultimate scattering will give the greatest polarization. Waves that entered the horizon before penultimate

scattering will still contribute, but not as much. Shorter wavelengths having lesser impact.

The final expression for the magnetic and electric polarization spectra eq. 142 contains a numerical factor $\frac{1}{16\pi}\left(\frac{1}{17}\ln\frac{20}{3}\right)^2$. Without the extra damping factor that appeared in the second order approximation of [1] this factor would be $\frac{1}{16\pi}\left(\frac{1}{7}\ln\frac{10}{3}\right)^2$ (B). The expression also contains the damping factor $D^2(k)$ which depends on the parameter $\alpha \in [0,2]$, the width of the decoupling $\Delta\eta_d^2$, the amplitude of the time derivative of the gravitational waves $|\dot{h}(\eta_d)|^2$ and a combination of spherical Bessel functions $j_l(k(\eta_d - \eta_0))$. Different features of the universe influence these parts in different ways, and thereby cause different changes in the polarization spectra.

To determine C_l^{XX} the initial amplitude of $\dot{h}(\eta_d)$ is necessary, but this depends on the ratio between the tensor and scalar perturbations r [1],

$$r = \frac{P_h(k_0)}{P_R(k_0)}. \tag{145}$$

The ratio is yet undetermined by observations, but some constraint has been given by the observation of the temperature anisotropies, which is generated both from scalar and tensorial perturbations. The third year report from WMAP limits $r < 0.22$ at 95% C.L. and $r < 0.37$ at 99.9% C.L. [1]. Here, r is taken as a parameter and the power spectra dependence on r is examined. WMAP observations indicates that the power spectrum of scalar perturbations is

$$P_R(k_0) = 2.95 \times 10^{-9} A(k_0) \tag{146}$$

with pivot wavenumber $k_0 = 0.05\ Mpc^{-1}$ and amplitude $A(k_0) \simeq 0.8$ [1]. With a RGW spectrum index $n_T = 0$ (scale-invariant), the amplitude from eq. 79 $A_T = 2.95 \times 10^{-9} A(k_0) r$. A smaller r yields a smaller amplitude A_T and greater difficulties in detecting the CMB polarization.

9.1 The Effect of the Visibility Function

The electric and magnetic type of power spectrum, C_l^{GG} and C_l^{CC}, calculated from eq. 142 and the numerical results from cmbfast, with tensor to scalar ratio $r = 1$, can be seen in fig. 7 and 8 [1]. The first and highest peak of the spectra can be found around $l \simeq 100$. The figures include both the result using the Gaussian and the half-Gaussian approximation for the visibility function, leading to the two different damping factors $D(k)$, eq. 141 and 140. C_l^{CC} and C_l^{GG} have a high sensitivity to the visibility function, i.e. to $D(k)$, at large l implying that $D(k)$ is more significant at small scales. A larger α causes a heavier damping. In the half-Gaussian approximation, C_l^{CC} for $\alpha = 1.7$ fits the numerical results well at the third peak, but are a bit too high for the second one, while $\alpha = 2$ is good at the second peak but too low at the third. Both the Gaussian and half-Gaussian approximations yields a too low power spectrum. Comparing them, with the same α, shows that the Gaussian visibility function gives a greater damping than the half-Gaussian. This is because $e^{-\alpha(k\Delta\eta_d)} < 1/2(e^{-\alpha(k\Delta\eta_{d1})} + e^{-\alpha(k\Delta\eta_{d2})})$ in

the region where the wavenumber k is sufficiently large for the $D(k)$ term to have a noticeable effect.

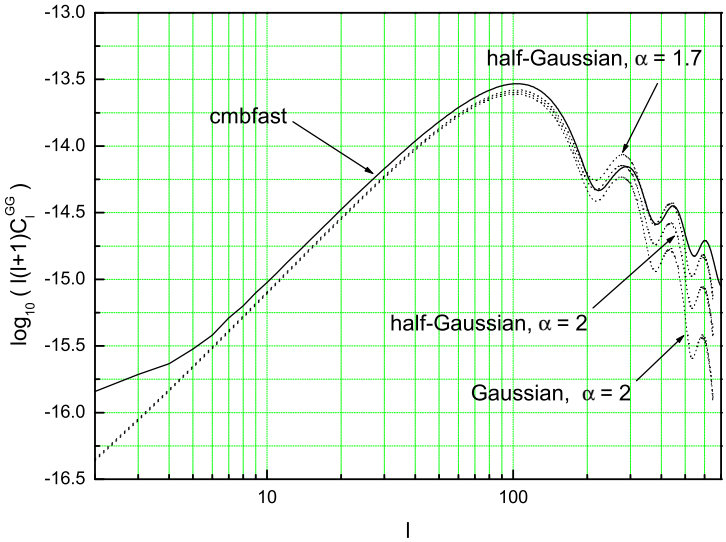

Fig. 7: The electric polarization spectrum C_l^{GG}. Numerical results from cmbfast code (solid line), results using half-Gaussian with $\alpha = 1.7, 2$ and Gaussian approximation with $\alpha = 2$ (dotted lines). Figure from [1].

9.2 The Dependence on Tensor/Scalar Ratio

The analytic expression (142) shows that $C_l^{XX} \propto |\dot{h}(\eta_d)|^2$. In a scale invariant universe ($n_T \simeq 0$), $|\dot{h}(\eta_d)|$ is directly related to the tensor/scalar ratio r. Fig. 9 shows the magnetic polarization power spectrum C_l^{CC} with three different values $r = 0.3,\ 0.1,\ 0.01$ as well as estimates of the sensitivity of WMAP and Planck (one-sigma sensitivity estimates). The WMAP estimate is based on noise measured during 8 years of operation, while the Planck estimate is based on 1.2 year of testing with a prototype [1] (Planck is planned to be launched on July 31st 2008 [22]). As seen in fig. 9 any detection of the magnetic polarization spectrum from the WMAP would be highly unlikely, but Planck should be able to observe C_l^{CC} from RGWs for $r > 0.1$.

The effect of reionization was left outside our analytic derivation. It will cause another peak in the visibility function, long after the decoupling, and give an additional contribution to the power spectra. Results from WMAP indicate that the reionization has an optical depth $\kappa_r = 0.09 \pm 0.03$ [10]. Numerical calculations using cmbfast include this effect and it can be observed as the first peak at low l in fig. 10 [1].

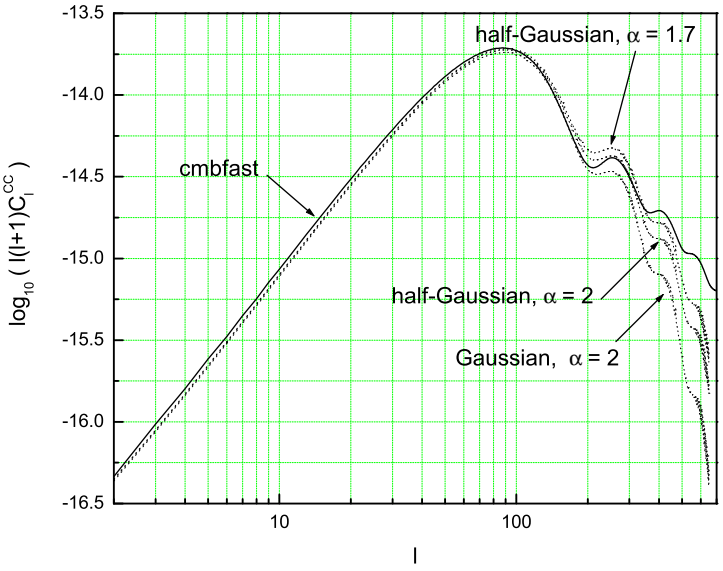

Fig. 8: The magnetic polarization spectrum C_l^{CC}. Numerical results from cmbfast code (solid line), results using half-Gaussian with $\alpha = 1.7$, 2 and Gaussian approximation with $\alpha = 2$ (dotted lines). Figure from [1].

9.3 Dependence on the Baryon Density

C_l^{XX} depends directly on the width of the decoupling, $\Delta\eta_d$, but also on the damping factor $D(k)$, which in turn depends on $\Delta\eta_d$. At very large scales (very small l) the effect of $D(k)$ is neglectable and a smaller $\Delta\eta_d$ will cause a lower spectrum. When the scale is smaller (large l) the contribution of $D(k)$ can no longer be ignored. For a fixed k, $D(k) = \frac{1}{2}(e^{-\alpha(k\Delta\eta_{d1})^2} + e^{-\alpha(k\Delta\eta_{d1})^2})$ grows when $\Delta\eta_d$ decrease, causing a more complex dependence. The total effect is determined by $C_l^{XX} \propto \Delta\eta_d^2 D^2(k)$.

The decoupling speed is mainly determined by the baryon density Ω_b. In the flat ΛCDM universe a larger Ω_b will increase the decoupling speed and $\Delta\eta_d$ will be smaller. A fitting function for the optical depth is

$$\kappa(z) = \Omega_b^{c_1} \left(\frac{z}{1000}\right)^{c_2} \tag{147}$$

where $c_1 = 0.43$ and $c_2 = 16 + 1.8\ln(\Omega_b)$.[1]

A larger Ω_b causes a larger κ and therefore a more localized visibility function $V(\eta)$ and a smaller $\Delta\eta_d$. The influence of Ω_b on $V(\eta)$ can be seen in fig. 11. Fig. 12 shows the influence of Ω_b on the magnetic polarization spectrum. Where a larger density, i.e. a shorter decoupling time, gives a lower spectrum.

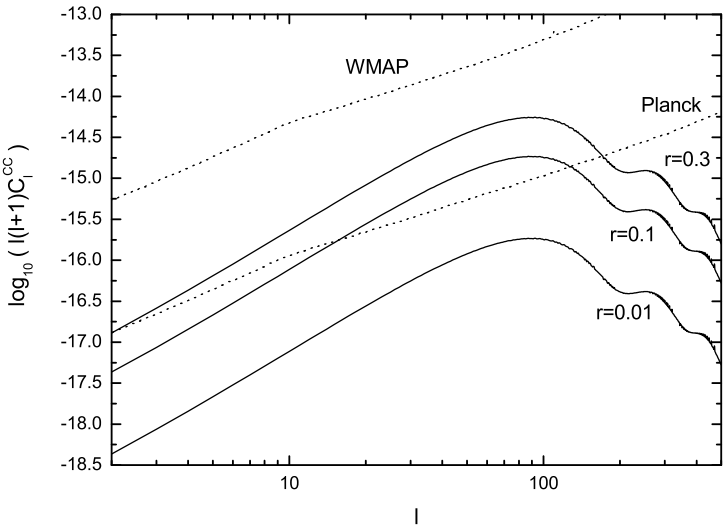

Fig. 9: The analytic magnetic polarization spectrum C_l^{CC} with tensor to scalar ratio $r = 0.3,\ 0.1,\ 0.01$ in the ΛCDM universe with $\Omega_b = 0.044$, $\Omega_d m = 0.226$ and $\Omega_\Lambda = 0.73$. Dotted lines are WMAP and Planck satellite sensitivity estimates for measuring the CMB magnetic polarization signal. Figure from [1]

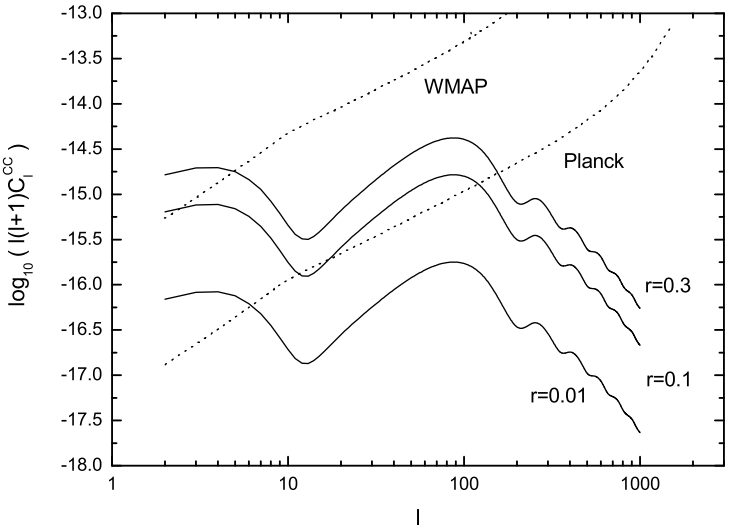

Fig. 10: The numerical magnetic polarization spectrum C_l^{CC} with tensor to scalar ratio $r = 0.3,\ 0.1,\ 0.01$ in the ΛCDM universe with $\Omega_b = 0.044$, $\Omega_d m = 0.226$ and $\Omega_\Lambda = 0.73$. Dotted lines are WMAP and Planck satellite sensitivity estimates for measuring the CMB magnetic polarization signal. Figure from [1]

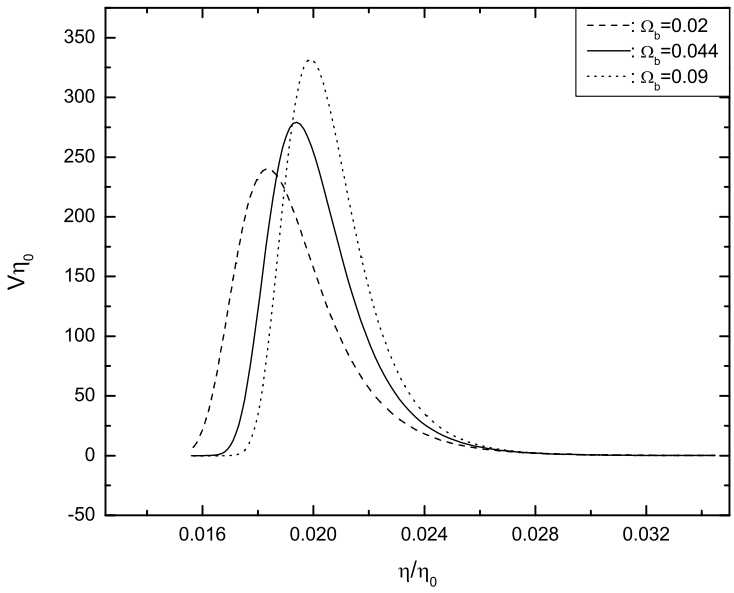

Fig. 11: Dependence of the visibility function $V(\eta)$ on the baryon density Ω_b in the ΛCDM universe with $\Omega_\Lambda = 0.73$ and $\Omega_{dm} = 1 - \Omega_\Lambda - \Omega_b$. Figure from [1].

9.4 Location of the Peaks

The C_l^{XX} spectrum peak at $l \simeq 100$, fig. 7 and 8. $P_{Gl}^2(k(\eta_d - \eta_0))$, eq. 143, and $P_{Cl}^2(k(\eta_d - \eta_0))$, eq. 144, are combinations of spherical Bessel functions $j_l(k(\eta_d - \eta_0))$. Their graphs for $l = 100$ can be seen in fig. 13 and 14 respectively.

The spherical Bessel functions $j_l(x)$, $x >> 1$ peaks about $l \simeq x$ [1]. Therefore $j_l(k(\eta_d - \eta_0))$ peaks around $l \simeq k(\eta_d - \eta_0) \simeq k\eta_0$ for $l >> 1$. Fig. 13 shows that P_{Gl} peaks at $k\eta_0 \simeq l$ and fig. 14 shows that P_{Cl} peaks at $k\eta_0 \simeq 1.27l$. This implies that the peak location of the polarization power spectrum is given by

$$C_l^{XX} \propto |\dot{h}(\eta_d)|^2 k^2 D^2(k)|_{k=l/\eta_0}. \tag{148}$$

$D(k)$ causes a greater damping at larger l so the first peak has the highest amplitude. Studying the first peak, with $D(k) \approx 1$. Eq. 89 gives

$$|\dot{h}(\eta_d)|^2 = A_0^2 k^2 (\frac{\eta_e}{\eta_d})^2 \left|A_1 j_2(k\eta_d) + A_2 y_2(k\eta_d)\right|^2. \tag{149}$$

For RGWs with a wavelength comparable to the horizon size at decoupling ($l \sim 100$) $A_1 j_2(k\eta_d) >> A_2 y_2(k\eta_d)$ and the last term can be neglected. Therefore $|\dot{h}(\eta_d)|^2 \propto |A_1 j_2(k\eta_d)|^2$ and since $j_2(k\eta_d)$ peaks at $k\eta_d \simeq 3$, $|\dot{h}(\eta_d)|^2$ peaks at $k\eta_d \simeq 3$, thereby causing the C_l^{XX} to peak around

$$l \simeq k\eta_0 \simeq 3\eta_0/\eta_d. \tag{150}$$

A ΛCDM universe with $\eta_d/\eta_0 = 0.0195$ gives a value of $k\eta_0 \simeq 154$. This result is based on the sudden transition approximation of $a(\eta)$. Using the WKB approximation, numerical calculations show that $|\dot{h}(\eta_d)|^2 k^2$ peaks at $k\eta_0 \sim 127$, fig. 15, and the analytic results is approximately correct.

The value of η_d/η_0 is mainly determined by the dark energy, Ω_Λ, and the baryon density Ω_b. A larger Ω_Λ gives a larger η_0/η_d and a longer lifetime of the universe. This would increase l in eq. 150, giving a way to study the age of the universe through CMB polarization. [1]

The time evolution of the gravitational wave $\dot{h}(\eta)$ also depends on the dark energy, fig. 16. As seen in the figure, a larger Ω_Λ shifts the peaks of $\dot{h}(\eta)$ to smaller scales and thereby causing a shift of the peaks in the polarization spectrum C_l^{XX} to smaller scales, fig. 17.

The baryon density, Ω_b, also affect the decoupling time η_d. If Ω_Λ is held fixed a larger Ω_b increases η_d, causing a smaller $3\eta_d/\eta_0$ and the peaks of C_l^{XX} shifts slightly to larger scales, as can be seen in fig. 12.

9.5 Influence of the spectrum index

The spectrum index n_T influences the spectrum of both the magnetic and the electric type through $|\dot{h}(\eta_d)|^2$. Fig. 18 show the electric spectrum with three different values, $n_T = -0.1,\ 0.0,\ 0.1$. A larger value corresponding to a higher spectrum. This is because $|\dot{h}(\eta_d)|^2$ differs from zero only at larger $k\eta_0$, fig. 3, and $|\dot{h}(\eta_d)| \propto k|h(\eta_d)|$ and $k^3|h(\eta_d)|^2 \propto k^{n_T}$. For a large k, a larger n_T causes a larger $|\dot{h}(\eta_d)|$ and a stronger polarization power spectrum C_L^{XX}.

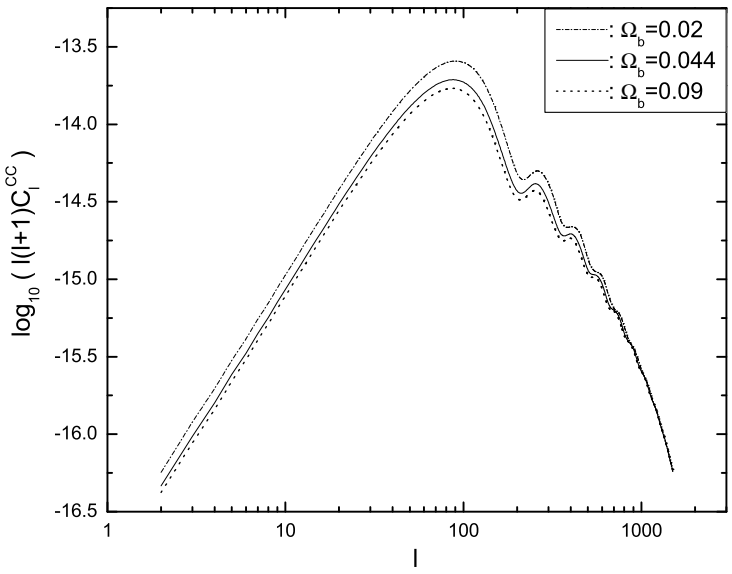

Fig. 12: Dependence of the magnetic polarization spectrum C_l^{CC} on the baryon density in ΛCDM universe with $\Omega_\Lambda = 0.73$ and $\Omega_{dm} = 1 - \Omega_\Lambda - \Omega_b$ and $r = 1$. Figure from [1].

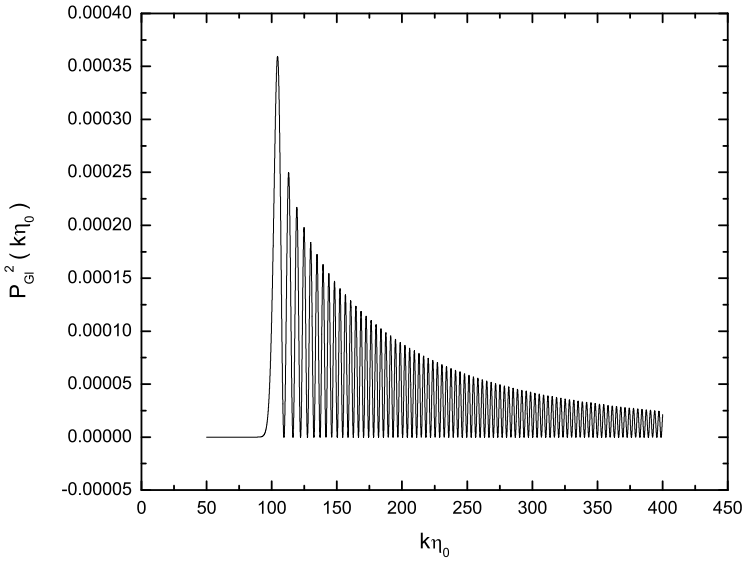

Fig. 13: $P^2_{Gk}(k)$ with $l = 100$ as a function of wavenumber k. Peaked around $k\eta_0 \sim 100$. Figure from [1].

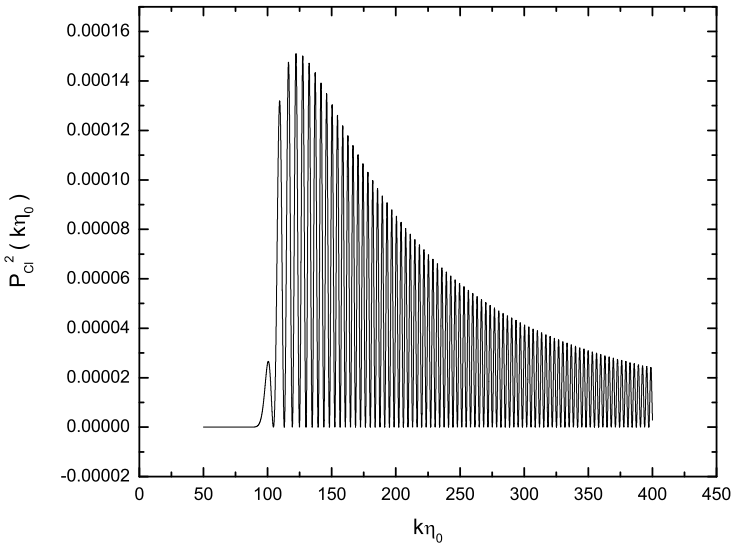

Fig. 14: $P^2_{Ck}(k)$ with $l = 100$ as a function of wavenumber k. Peaked around $k\eta_0 \sim 127$. Figure from [1].

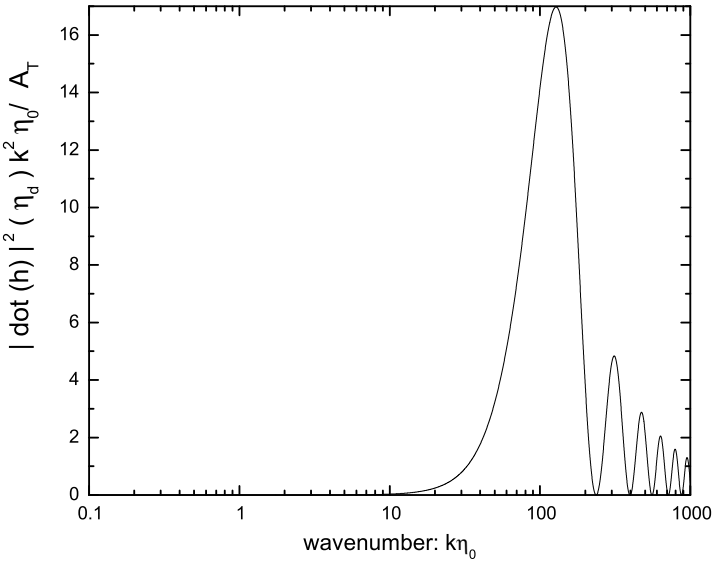

Fig. 15: $|\dot{h}(\eta_d)|^2 k^2 \eta_0 / A_T$ as a function of wavenumber k in the WKB approximation of the scale factor $a(\eta)$. The function peaks around $k\eta_0 \sim 127$. Figure from [1].

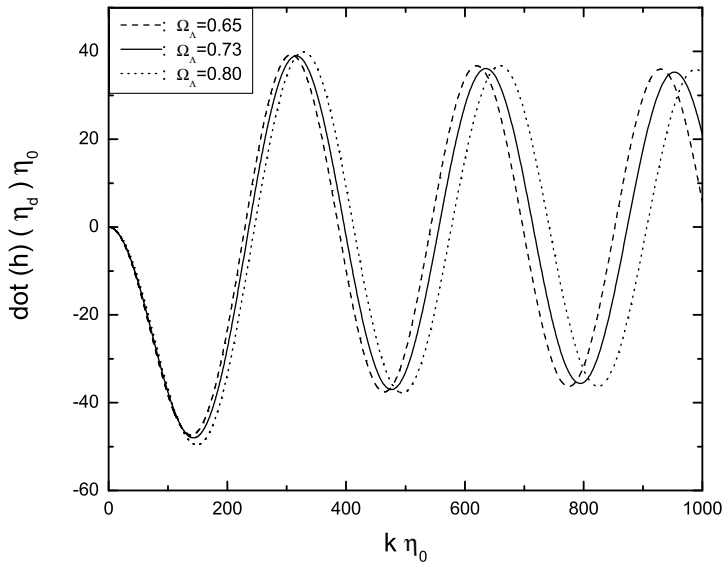

Fig. 16: The effect of the dark energy Ω_Λ on the time evolution of RGWs $\dot{h}(\eta)$. A larger Ω_Λ shifts the graph to smaller scales. Figure from [1].

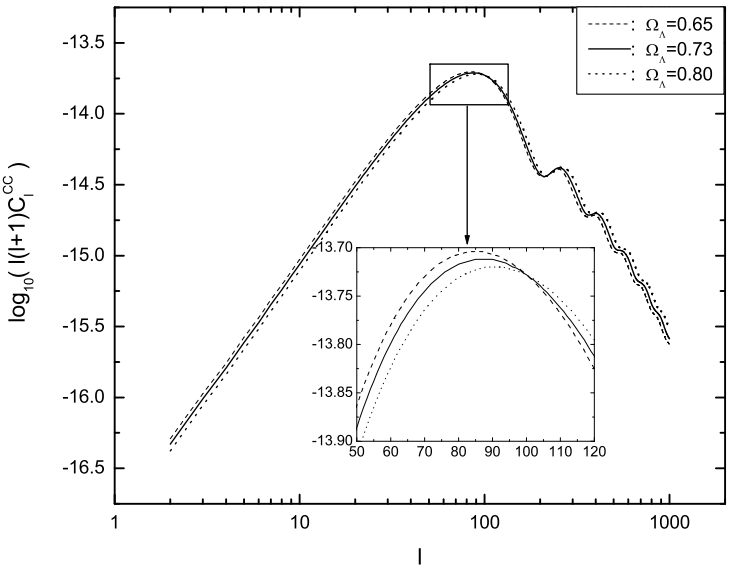

Fig. 17: The effect of dark energy Ω_{Lambda} on the magnetic polarization spectrum C_l^{CC}. A larger Ω_Λ shifts the peaks slightly to smaller scales and lower the amplitude. Figure from [1].

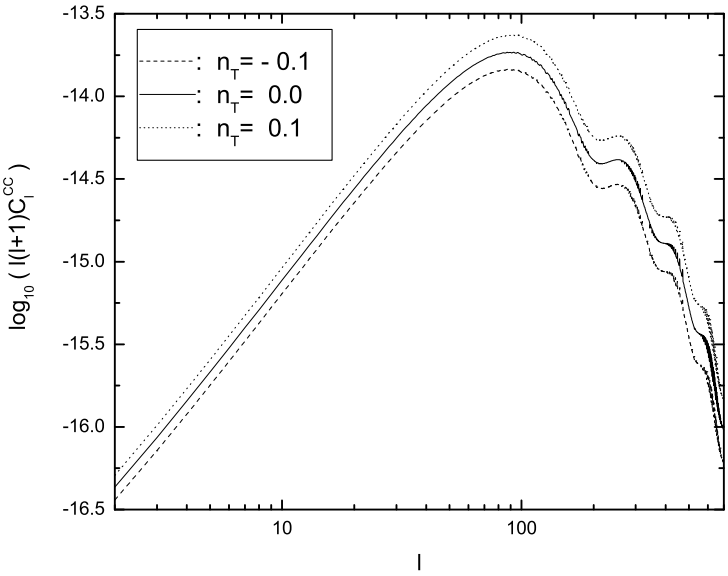

Fig. 18: Dependence of the magnetic polarization C_l^{CC} spectrum on the spectrum index n_T in ΛCDM universe, $r = 1$ and $\alpha = 2$ in the half-Gaussian fitting. A larger n_T gives a higher spectrum. Figure from [1].

10 Conclusions

The effect on the polarization in the CMB from metric perturbations due to gravitational waves has been studied analytically in this thesis. The polarization caused by metric perturbations induced by relic gravitational waves are different from those induced by scalar perturbations. The derived analytic expression has qualitatively explained the features of the polarization spectra obtained by more exact numerical calculations and give an insight in the physics behind.

The greatest cause of polarization arise due to the gravitational waves that enter the horizon between penultimate and last scattering. The polarization spectra have a strong dependence on the width of decoupling and thereby the visibility function at that time. Also, the derivations have shown that including the effect of photon diffusion, i.e. the second order of the tight coupling, does not produce an extra, wavenumber independent damping factor.

The dependence of the spectra on different cosmological parameters give the CMB polarization measurements a position as one of the key projects of astrophysics and cosmology. Measurements of polarization in the CMB might soon be within observational reach and the results, weather they are detected or not, will constrain theories about the development in the early universe. Therefore the analytical insight in the physics causing this polarization is important.

Acknowledgements

First and foremost I would like to thank my supervisor Johan Bijnens, whom I could not have completed this thesis without. For his support, many useful explanations and razor sharp ability to see where trouble arise, long before I notice them myself.

I would also like to thank all friends and family that have put up with me and my rambling about gravitational waves, providing me with use full critisism and questions. Some ones that deserve to be mentioned are Anders Svensson, Niclas Svensson, Peter Johansson Johan Persson and Marianne Döös.

Finally, I should not forget all the people at the Theoretical Physics Department for creating a great atmosphere and a source of inspiration.

A Appendix

A.1 Transverse-Traceless Gauge

This section is only valid in Minkowski space, with a metric tensor $g_{\alpha\beta} = \eta_{\alpha\beta} + h_{\alpha\beta}$ where $\eta_{\alpha\beta}$ is the Minkowski spacetime and the scale factor $a(\eta) = 1$. The different convention with the minus sign in front of the time part of the metric is used and time is denoted by t. However, locally one can always work in a Minkowski space thus the result should hold for gravitational waves of short enough wavelengths for the Minkowski approximation to be good.

Einstein's equation in vacuum is [4]

$$\left(-\frac{\partial^2}{\partial t^2}+\nabla^2\right)\bar{h}^{\alpha\beta}=0 \tag{151}$$

Where $\bar{h}^{\alpha\beta}$ is the trace reverse of $h_{\alpha\beta}$,

$$\bar{h}^{\alpha\beta}=h^{\alpha\beta}-\frac{1}{2}\eta^{\alpha\beta}h. \tag{152}$$

$\eta^{\alpha\beta}$ is here the metric of a flat universe. Eq. 151 has a solution of the form

$$\bar{h}^{\alpha\beta}=A^{\alpha\beta}e^{ik_\mu x^\alpha}. \tag{153}$$

This implies that

$$\bar{h}^{\alpha\beta}_{\mu}=k_\mu\bar{h}^{\alpha\beta}. \tag{154}$$

Combining with $\bar{h}^{\alpha\beta}_{,\beta}=0$ gives

$$A^{\alpha\beta}k_\beta=0, \tag{155}$$

meaning that the amplitudes of the gravitational wave must be orthogonal to the direction of propagation, $\hat{k}$. Using the gauge freedom to choose the transverse-traceless gauge imposing the two more conditions on the amplitude

$$A^\alpha_\alpha=0 \tag{156}$$

and

$$A_{\alpha\beta}U^\beta=0 \tag{157}$$

where U^β is any fixed four momentum, i.e. any constant timelike vector. The first condition implies that $\bar{h}^{\alpha\beta}=h^{\alpha\beta}$. While the second condition together with the previous orthogonality one implies that

$$A^{TT}_{\alpha\beta}=\begin{pmatrix}0&0&0&0\\0&A_{xx}&A_{xy}&0\\0&A_{xy}&-A_{xx}&0\\0&0&0&0\end{pmatrix} \tag{158}$$

It is then obvious that there can only be two independent polarizations modes of gravitational waves. These two correspond to the h^+ and $h^\times$ polarizations.

A.2 Base Functions for Thomson Scattering

The perturbed radiation $\mathbf{a}=(1-\mu'^2)\cos 2(\phi'-\phi)\begin{pmatrix}1\\1\\0\end{pmatrix}$ is Thomson scattered,

$$J = \frac{1}{4\pi}\int_{-1}^{1}d\mu'\int_0^{2\pi}d\phi'\times$$

$$\begin{pmatrix} \mu^2\mu'^2\cos 2(\phi'-\phi) & -\mu^2\cos 2(\phi'-\phi) & \mu^2\mu'^2\sin 2(\phi'-\phi) \\ -\mu'^2\cos 2(\phi'-\phi) & \cos 2(\phi'-\phi) & -\mu'\sin 2(\phi'-\phi) \\ -2\mu\mu'^2\sin 2(\phi'-\phi) & 2\mu\sin 2(\phi'-\phi) & 2\mu\mu'\cos 2(\phi'-\phi) \end{pmatrix} \times$$
$$(1-\mu'^2)\cos 2\phi' \begin{pmatrix} 1 \\ 1 \\ 0 \end{pmatrix}$$
$$= \frac{3}{32}\int_{-1}^{1} d\mu'(1-\mu'^2) \begin{pmatrix} \mu^2\mu'^2\cos 2\phi & -\mu^2\cos 2\phi & 0 \\ -\mu'^2\cos 2\phi & \cos 2\phi & 0 \\ -2\mu\mu'^2\sin 2\phi & 2\mu\sin 2\phi & 0 \end{pmatrix}$$
$$= \frac{1}{320}\begin{pmatrix} -16\mu^2\cos 2\phi \\ 16\cos 2\phi \\ -32\mu\sin 2\phi \end{pmatrix}$$
$$= \frac{1}{20}(\mathbf{a}-\mathbf{b}), \tag{159}$$

where

$$\mathbf{b} = \frac{1}{2}\begin{pmatrix} (1+\mu^2)\sin 2\phi \\ -(1+\mu^2)\sin 2\phi \\ 4\mu\cos 2\phi \end{pmatrix}. \tag{160}$$

Similar calculations lead to essentially the same results for the $h^{\times}$ polarization. Hence, as radiation polarized by RGWs undergo Thomson scattering the polarization is changed to a linear combination of $\tilde{a}$ and $\tilde{b}$.

A.3 Sachs-Wolfe Effect

The derivation of the Sachs-Wolfe effect in the FRW-universe to first order in the perturbations. The Geodesic Equation is

$$\frac{d^2x^\mu}{d\lambda^2} = -\Gamma^\mu_{\alpha\beta}\frac{dx^\alpha}{d\lambda}\frac{dx^\beta}{d\lambda}. \tag{161}$$

For a photon

$$g_{\mu\nu}P^\mu P^\nu = 0 \tag{162}$$

and

$$\frac{d}{d\lambda} = \frac{dx^0}{d\lambda}\frac{d}{dx^0} = \frac{d\eta}{d\lambda}\frac{d}{d\eta} = P^0\frac{d}{d\eta}. \tag{163}$$

P^0 is the photon energy, which is constant in an unperturbed universe, multiplied by the scale factor a. [2] The perturbed metric is

$$ds^2 = g_{\mu\nu}dx^\mu dx^{nu} = a^2\left[d\eta^2 - (\delta_{ij}+h_{ij})dx^i dx^j\right]. \tag{164}$$

Taking the 0's component of the geodesic equation, the left hand side is

$$\frac{d^2x^0}{d\lambda^2} = \frac{d}{d\lambda}P^0 = P^0\frac{d}{d\eta}P^0 = \frac{1}{a^2}P_0\frac{d}{d\eta}\left(\frac{1}{a^2}P_0\right)$$
$$= \frac{1}{a^4}P_0\left(\frac{d}{d\eta}P_0 - \frac{2}{a}P_0\frac{d}{d\eta}a\right). \tag{165}$$

For the right hand side the Christoffel symbols are needed,

$$\Gamma^{\mu}_{\beta\alpha} = \frac{1}{2} g^{\mu\nu} \left(g_{\nu\alpha,\beta} + g_{\nu\beta,\alpha} + g_{\alpha\beta,\nu} \right) \tag{166}$$

$$\Rightarrow \begin{cases} \Gamma^0_{00} = \frac{1}{2a^2} g_{00,0} = \frac{1}{2a^2} \frac{d}{d\eta} a^2 \\ \Gamma^0_{ii} = \frac{1}{2a^2} g_{ii,0} = \frac{1}{2a^2} \frac{d}{d\eta} a^2 (1 + h_{ii}) \\ \Gamma^0_{ij} = \Gamma^0_{ji} = \frac{1}{2a^2} \frac{d}{d\eta} a^2 (h_{ij}) \quad \forall i \neq j \end{cases} . \tag{167}$$

Thus, with $\mu = 0$

$$\begin{aligned} -\Gamma^{\mu}_{\alpha\beta} \frac{dx^\alpha}{d\lambda} \frac{dx^\beta}{d\lambda} &= -\Gamma^0_{00} (P^0)^2 - \Gamma^0_{xx} (P^x)^2 - \Gamma^0_{yy} (P^y)^2 - \Gamma^0_{zz} (P^z)^2 \\ &\quad -2\Gamma^0_{xy} P^x P^y - 2\Gamma^0_{xz} P^x P^z - 2\Gamma^0_{yz} P^y P^z \\ &= -\frac{1}{2a^2} \left[(P^0)^2 \frac{d}{d\eta} a^2 + P^i P^j \frac{d}{d\eta} a^2 (1 + h_{ij}) \right] \\ &= -\frac{1}{2a^2} \left[(P^0)^2 \frac{d}{d\eta} a^2 + P^i P^j (1 + h_{ij}) \frac{d}{d\eta} a^2 + P^i P^j a^2 \frac{d}{d\eta} h_{ij} \right] \\ &= -\frac{1}{a^2} (P^0)^2 \frac{d}{d\eta} a^2 - \frac{1}{2} P^i P^j \frac{d}{d\eta} h_{ij}, \end{aligned} \tag{168}$$

where

$$0 = g_{\mu\nu} P^\mu P^\nu = a^2 \big((P^0)^2 - \delta_{ij} P^i P^j - h_{ij} P^i P^j \big) \tag{169}$$

and

$$(P^0)^2 = \delta_{ij} P^i P^j + h_{ij} P^i P^j \tag{170}$$

have been used in the last equality. The first term on the RH side cancels out the second term in the LH side and what's left is

$$\frac{1}{a^4} P_0 \frac{d}{d\eta} P_0 = -\frac{1}{2} \frac{dh_{ij}}{d\eta} P^i P^j. \tag{171}$$

On the RH side there already is one power of h_+, thus to first order

$$P^\mu = \big(P^0, P^0 \sin\theta \sin\phi, P^0 \sin\theta \cos\phi, P^0 \cos\theta \big) \tag{172}$$

Which gives us

$$\frac{1}{P_0} \frac{d}{d\eta} P_0 = -\frac{1}{2} \frac{dh_{ij}}{d\eta} \frac{P^i P^j}{(P^0)^2} = -\frac{1}{2} \frac{dh_{ij}}{d\eta} \hat{n}^i \hat{n}^j. \tag{173}$$

Substituting P_0 with the frequency yields the general expression for the Sachs-Wolfe effect,

$$\frac{1}{\nu} \frac{d\nu}{d\eta} = \frac{1}{2} \frac{\partial h_{ij}}{\partial \eta} \hat{n}^i \hat{n}^j. \tag{174}$$

A.4 Coupled Differential Equations

A.4.1 Unperturbed Radiation

Examining the Boltzmann equation, eq. 45 for the unperturbed radiation, i.e. f_0.

$$f_0 = \frac{1}{e^{h\nu/kT} - 1} \tag{175}$$

$$\frac{\partial f_0}{\partial \eta} = 0 \tag{176}$$

since f_0 is independent of the conformal time.

$$\frac{\partial f_0}{\partial x^i} = 0 \tag{177}$$

since there is no explicit dependence on any spatial coordinate. The part originating from the Thomson scattering $q[f - J]$ equals zero because due to the spherical symmetry of the scattering matrix

$$J(f_0) = f_0 \tag{178}$$

and in the unperturbed part there is no gravitational perturbation so the gravitational term vanishes as well.

A.4.2 Perturbed Radiation

Specializing eq. 62 to the case of RGWs with h^+ polarization by substituting f_1 in eq. 58.

$$\begin{aligned}
&\frac{1}{2}\cos 2\phi(1-\mu^2)\begin{pmatrix}1\\1\\0\end{pmatrix}(\dot{\zeta}_k + ik\mu\zeta_k) + \frac{1}{2}\begin{pmatrix}(1+\mu^2)\cos 2\phi\\-(1+\mu^2)\cos 2\phi\\4\mu\sin 2\phi\end{pmatrix}(\dot{\beta}_k + ik\mu\beta_k)\\
= \;& -\frac{1}{2}\frac{v}{f_0}\frac{\partial f_0}{\partial \nu_0}(1-\mu^2)\cos 2\phi\frac{dh_k(\eta)}{d\eta}\\
& -q(\eta)\frac{1}{2}\left[\zeta_k(1-\mu^2)\begin{pmatrix}1\\1\\0\end{pmatrix}\cos 2\phi + \beta_k\begin{pmatrix}(1+\mu^2)\cos 2\phi\\-(1+\mu^2)\cos 2\phi\\4\mu\sin 2\phi\end{pmatrix}\right] + q\tilde{J}.
\end{aligned} \tag{179}$$

Moving all the terms containing ζ_k or β_k to the LH side, the result is,

$$\begin{aligned}
&\frac{1}{2}\cos 2\phi(1-\mu^2)\begin{pmatrix}1\\1\\0\end{pmatrix}(\dot{\zeta}_k + ik\mu\zeta_k) + \frac{1}{2}\begin{pmatrix}(1+\mu^2)\cos 2\phi\\-(1+\mu^2)\cos 2\phi\\4\mu\sin 2\phi\end{pmatrix}(\dot{\beta}_k + ik\mu\beta_k)\\
&-q(\eta)\frac{1}{2}\left[\zeta_k(1-\mu^2)\begin{pmatrix}1\\1\\0\end{pmatrix}\cos 2\phi + \beta_k\begin{pmatrix}(1+\mu^2)\cos 2\phi\\-(1+\mu^2)\cos 2\phi\\4\mu\sin 2\phi\end{pmatrix}\right]\\
&= -\frac{1}{2}\frac{v}{f_0}\frac{\partial f_0}{\partial \nu_0}(1-\mu^2)\cos 2\phi\frac{dh_k}{d\eta} + q\tilde{J}.
\end{aligned} \tag{180}$$

This gives three different equations:

$$(1-\mu^2)\dot{\zeta}_k + (1+\mu^2)\dot{\beta}_k + (ik\mu+q)\left[(1-\mu^2)\zeta_k + (1+\mu^2)\beta_k\right] = -(1-\mu^2)\frac{v}{f_0}\frac{\partial f_0}{\partial \nu_0}\frac{dh_k}{d\eta} + \frac{2q}{\cos 2\phi}J_1 \tag{181}$$

$$(1-\mu^2)\dot{\zeta}_k - (1+\mu^2)\dot{\beta}_k + (ik\mu+q)\left[(1-\mu^2)\zeta_k - (1+\mu^2)\beta_k\right] = -(1-\mu^2)\frac{v}{f_0}\frac{\partial f_0}{\partial \nu_0}\frac{dh_k}{d\eta} + \frac{2q}{\cos 2\phi}J_2 \tag{182}$$

$$4\mu\sin 2\phi\left[\dot{\beta}_k + (ik\mu+q)\beta_k\right] = \cos 2\phi[-(1-\mu^2)\frac{v}{f_0}\frac{\partial f_0}{\partial \nu_0}\frac{dh_k}{d\eta} + 2qJ_3]. \tag{183}$$

$\tilde{J}$ is given by eq. 46.

$$\begin{aligned}
\tilde{J} &= \frac{3}{16\pi}\int_{-1}^{1}d\mu'\int_0^{2\pi}d\phi'\times \\
&\quad \begin{pmatrix} \mu^2\mu'^2\cos 2(\phi'-\phi) & -\mu^2\cos 2(\phi'-\phi) & \mu^2\mu'\sin 2(\phi'-\phi) \\ -\mu'^2\cos 2(\phi'-\phi) & \cos 2(\phi'-\phi) & -\mu'\sin 2(\phi'-\phi) \\ -2\mu\mu'^2\sin 2(\phi'-\phi) & 2\mu\sin 2(\phi'-\phi) & 2\mu\mu'\cos 2(\phi'-\phi) \end{pmatrix}\times \\
&\quad \left[\frac{\zeta_k}{2}(1-\mu'^2)\cos 2\phi'\begin{pmatrix}1\\1\\0\end{pmatrix} + \frac{\beta_k}{2}\begin{pmatrix}(1+\mu'^2)\cos 2\phi'\\-(1+\mu'^2)\cos 2\phi'\\4\mu'\sin 2\phi'\end{pmatrix}\right] \\
&= \frac{3}{16\pi}\int_{-1}^{1}d\mu'\pi\begin{pmatrix} \mu^2\mu'^2\cos 2\phi & -\mu^2\cos 2\phi & \mu^2\mu'\cos 2\phi \\ -\mu'^2\cos 2\phi & \cos 2\phi & -\mu'\cos 2\phi \\ 2\mu\mu'^2\sin 2\phi & -2\mu\sin 2\phi & 2\mu\mu'\sin 2\phi \end{pmatrix}\times \\
&\quad \left[\frac{\zeta_k}{2}(1-\mu'^2)\begin{pmatrix}1\\1\\0\end{pmatrix} + \frac{\beta_k}{2}\begin{pmatrix}(1+\mu'^2)\\-(1+\mu'^2)\\4\mu'\end{pmatrix}\right],
\end{aligned} \tag{184}$$

here

$$\int_0^{2\pi}\cos 2(\phi'-\phi)\cos 2\phi' d\phi' = \pi\cos 2\phi, \tag{185}$$

$$\int_0^{2\pi}\sin 2(\phi'-\phi)\cos 2\phi' d\phi' = -\pi\sin 2\phi, \tag{186}$$

$$\int_0^{2\pi}\cos 2(\phi'-\phi)\sin 2\phi' d\phi' = \pi\sin 2\phi, \tag{187}$$

$$\int_0^{2\pi}\sin 2(\phi'-\phi)\sin 2\phi' d\phi' = \pi\cos 2\phi \tag{188}$$

was used. This leads to the different J's:

$$J_1 = \frac{3}{32}\mu^2\cos 2\phi\int_{-1}^{1}d\mu'[-(1-\mu'^2)^2\zeta_k + (1+\mu'^2)^2\beta_k + 4\mu'^2\beta_k] = \frac{3}{16}\mu^2\cos 2\phi I \tag{189}$$

$$J_2 = \frac{3}{32}\cos 2\phi \int_{-1}^{1} d\mu'[(1-\mu'^2)^2\zeta_k - (1+\mu'^2)^2\beta_k - 4\mu'^2\beta_k]$$
$$= -\frac{3}{16}\cos 2\phi I \tag{190}$$

$$I(\eta,k) = \int_{-1}^{1} d\mu'[(1+\mu'^2)^2\beta_k - \frac{1}{2}(1-\mu'^2)^2(\zeta_k+\beta_k)] \tag{191}$$

Plugging this into eq. 181 and 182:

$$(1-\mu^2)\dot{\zeta}_k + (1+\mu^2)\dot{\beta}_k + (ik\mu+q)\left[(1-\mu^2)\zeta_k + (1+\mu^2)\beta_k\right]$$
$$= -(1-\mu^2)\frac{v}{f_0}\frac{\partial f_0}{\partial \nu_0}\frac{dh_k}{d\eta} + \frac{3q}{8}\mu^2 I \tag{192}$$

and

$$(1-\mu^2)\dot{\zeta}_k - (1+\mu^2)\dot{\beta}_k + (ik\mu+q)\left[(1-\mu^2)\zeta_k - (1+\mu^2)\beta_k\right]$$
$$= -(1-\mu^2)\frac{v}{f_0}\frac{\partial f_0}{\partial \nu_0}\frac{dh_k}{d\eta} - \frac{3q}{8} I \tag{193}$$

Multiplying eq. 193 by μ^2, adding it to eq. 192 and dividing by two to obtain eq. 195. Subtracting eq. 193 from eq. 192 leads to eq 194.

$$(1+\mu^2)\dot{\beta}_k + (ik\mu+q)(1+\mu^2)\beta_k = (1+\mu^2)\frac{3q}{16} I \tag{194}$$

$$\dot{\zeta}_k + \dot{\beta}_k + (ik\mu+q)(\zeta_k+\beta_k) = -\frac{v}{f_0}\frac{\partial f_0}{\partial \nu_0}\frac{dh_k}{d\eta} \tag{195}$$

Dividing the first one by $(1+\mu^2)$, define

$$\xi_k = \zeta_k + \beta_k \tag{196}$$

and note that

$$-\frac{v}{f_0}\frac{\partial f_0}{\partial \nu_0}\frac{dh_k}{d\eta} = \frac{d\ln f_0}{d\ln \nu_0}\dot{h}_k. \tag{197}$$

The result is

$$\dot{\beta}_k + (ik\mu+q)\beta_k = \frac{3q}{16} I \tag{198}$$

$$\dot{\xi}_k + (ik\mu+q)\xi_k = \frac{d\ln f_0}{d\ln \nu_0}\dot{h}_k \tag{199}$$

Repeating the calculations for $h^\times$ leads to the same result, so the $\dot{h}$ in eq. 199 can be either $\dot{h}^+$ and $\dot{h}^\times$. In the Rayleigh-Jeans zone $\frac{\ln f_0}{\ln \nu_0} \approx 1$ [1].

A.5 Curl and Divergence of Spherical Harmonics

The covariant derivatives of the spherical harmonics on the two sphere are

$$\left\{ \begin{array}{l} Y_{(lm):\theta\theta} = Y_{(lm),\theta\theta} \\ Y_{(lm):\theta\phi} = Y_{(lm):\phi\theta} = Y_{(lm),\theta\phi} - \cot\theta Y_{(lm),\phi} \\ Y_{(lm):\phi\phi} = Y_{(lm),\phi\phi} + \sin\theta\cos\theta Y_{(lm),\theta} \end{array} \right. \tag{200}$$

The divergence is therefore

$$\begin{aligned} Y_{(lm):c}^{\quad c} &= g^{\mu c} Y^{=}_{(lm):c\mu} g^{\theta\theta} Y_{(lm):\theta\theta} + g^{\phi\phi} Y_{(lm):\phi\phi} \\ &= Y_{(lm):\theta\theta} + \frac{1}{\sin^2\theta} Y_{(lm):\phi\phi} \end{aligned} \tag{201}$$

$$\begin{aligned} Y^G_{(lm)\theta\theta} &= N_l (Y_{(lm):\theta\theta} - \frac{1}{2} g_{\theta\theta} Y_{(lm):c}^{\quad c}) \\ &= \frac{N_l}{2} (Y_{(lm),\theta\theta} - \frac{Y_{(lm),\phi\phi}}{\sin^2\theta} - \cot\theta Y_{(lm),\theta}) \end{aligned} \tag{202}$$

$$Y^G_{(lm)\theta\phi} = Y^G_{(lm)\phi\theta} = N_l Y_{(lm)\theta\phi} \tag{203}$$

$$Y^G_{(lm)\phi\phi} = -\sin^2\theta Y^G_{(lm)\theta\theta} \tag{204}$$

and the curl is

$$\begin{aligned} Y^C_{(lm)\theta\theta} &= -2\frac{Y_{(lm):\theta\phi}}{\sin\theta} = \frac{-2m}{\sin\theta}(\partial_\theta - \cot\theta) Y_{(lm)} \\ Y^C_{(lm)\phi\phi} &= -2 Y_{(lm):\phi\theta} \sin\theta = 2m \sin\theta (\partial_\theta - \cot\theta) Y_{(lm)} \\ Y^C_{(lm)\phi\theta} &= Y^C_{(lm)\theta\phi} = Y_{(lm):\theta\theta}\sin\theta - \frac{Y_{(lm):\phi\phi}}{\sin\theta} \\ &= \left(\sin\theta\partial_\theta^2 - \frac{m^2}{\sin\theta} - \cos\theta\partial_\theta \right) Y_{(lm)} \end{aligned} \tag{205}$$

The divergence and curl of the spherical harmonics are

$$Y^G_{(lm)ab}(\hat{n}) = \frac{N_l}{2} \begin{pmatrix} W_{(lm)} & X_{(lm)}\sin\theta \\ X_{(lm)}\sin\theta & -W_{(lm)}\sin^2\theta \end{pmatrix} \tag{206}$$

and

$$Y^G_{(lm)ab}(\hat{n}) = \frac{N_l}{2} \begin{pmatrix} -X_{(lm)} & W_{(lm)}\sin\theta \\ W_{(lm)}\sin\theta & X_{(lm)}\sin^2\theta \end{pmatrix} \tag{207}$$

defining $W(\hat{n})$ and $X(\hat{n})$.

$$\begin{aligned} W_{(lm)}(\theta,\phi) &= \left(\partial_\theta^2 - \cot\theta\partial_\theta + \frac{m^2}{\sin^2\theta} \right) Y_{(lm)} \\ &= \left(-2\cot\theta\partial_\theta + 2\frac{m^2}{\sin^2\theta} - l(l+1) \right) Y_{(lm)} \end{aligned} \tag{208}$$

Expressing the spherical harmonics in Legendre polynomials

$$Y_{(lm)}(\theta,\phi)=\sqrt{\frac{(2l+1)}{4\pi}\frac{(l-m)!}{(l+m)!}}P_{(lm)}(\cos\theta)e^{im\phi} \tag{209}$$

and then using the recurrence relation [7]

$$-(1+\mu^2)\frac{dP_l^m(\mu)}{d\mu}=l\mu P_l^m-(l+m)P_{l-1}^m, \tag{210}$$

$$\begin{aligned}
W_{(lm)} &= 2\sqrt{\frac{(2l+1)}{4\pi}\frac{(l-m)!}{(l+m)!}}e^{im\phi}\left(-\cot\theta\partial_\theta+\frac{m^2}{\sin^2\theta}-\frac{l(l+1)}{2}\right)P_l^m \\
&= 2\sqrt{\frac{(2l+1)}{4\pi}\frac{(l-m)!}{(l+m)!}}e^{im\phi} \\
&\quad\times\Big[\frac{\mu}{\mu^2-1}\left(l\mu P_l^m-(l+m)P_{l-1}^m\right)+\frac{m^2}{1-\mu^2}P_l^2-\frac{l(l+1)}{2}P_l^2\Big] \\
&= 2\sqrt{\frac{(2l+1)}{4\pi}\frac{(l-m)!}{(l+m)!}}e^{im\phi} \\
&\quad\times\left[\frac{m-l}{\sin^2\theta}P_l^m+\frac{l(l-1)}{2}P_l^m+\frac{\cos\theta(l+m)}{\sin^2\theta}P_{l-1}^m\right].
\end{aligned} \tag{211}$$

Similarly

$$\begin{aligned}
X_{(lm)} &= \frac{i2m}{\sin\theta}(\partial_\theta-\cot\theta)Y_{(lm)}=2m(\partial_\mu+\cot\theta)Y_{(lm)} \\
&= -2im\sqrt{\frac{(2l+1)}{4\pi}\frac{(l-m)!}{(l+m)!}}e^{im\phi}(\partial_\mu+\cot\theta)P_l^m \\
&= 2\sqrt{\frac{(2l+1)}{4\pi}\frac{(l-m)!}{(l+m)!}}e^{im\phi}\left[\frac{\cos\theta}{\sin^2\theta}(l-1)P_l^m-\frac{(l+m)}{\sin^2\theta}P_{l-1}^m\right]
\end{aligned} \tag{212}$$

A.6 Expansion Coefficients

The expansion coefficients are given by:

$$a^G_{(lm)}=\frac{1}{T}\int d\hat{n}P_{ab}(\hat{n})Y^{G\,ab*}_{(lm)}(\hat{n}) \tag{213}$$

$$a^C_{(lm)}=\frac{1}{T}\int d\hat{n}P_{ab}(\hat{n})Y^{C\,ab*}_{(lm)}(\hat{n}) \tag{214}$$

where

$$Y^G_{(lm)ab}=N_l\left(Y_{(lm):ab}-\frac{1}{2}g_{ab}Y^c_{(lm):c}\right) \tag{215}$$

$$Y^C_{(lm)ab} = \frac{N_l}{2}\left(Y_{(lm):ac}\epsilon^c_b + Y_{(lm):bc}\epsilon^c_a\right) \tag{216}$$

where

$$N_l = \sqrt{2(l-2)!/(l+2)!} \tag{217}$$

and

$$P_{ab}(\hat{n}) = \frac{1}{2}\begin{pmatrix} Q(\hat{n}) & -U(\hat{n})\sin\theta \\ -U(\hat{n})\sin\theta & -Q(\hat{n})\sin^2\theta \end{pmatrix} \tag{218}$$

Integrating eq. 213 by parts to obtain

$$a^G_{(lm)} = \frac{N_l}{T_0}\int d\hat{n} Y^*_{(lm)} P_{ab}{}^{:ab} \tag{219}$$

and

$$a^C_{(lm)} = \frac{N_l}{T_0}\int d\hat{n} Y^*_{(lm)} P_{ab}{}^{:ac}\epsilon_c{}^b. \tag{220}$$

A.6.1 The Electric Type

The coefficient of the electric type of polarization $a^G_{(lm)}$.

$$\begin{aligned} P_{ab}{}^{:ab} = P^{ab}{}_{:ab} &= P^{\theta\theta}{}_{,\theta\theta} + 2P^{\theta\phi}{}_{\theta\phi} + P^{\phi\phi}{}_{\phi\phi} - \sin\theta\cos\theta P^{\phi\phi}_{\theta} + 2\cot\theta P^{\theta\theta}_{\theta} \\ &\quad +4\cot\theta P^{\theta\phi}_{\phi} + (1-3\cos^2\theta)P^{\phi\phi} - P^{\theta\theta}. \end{aligned} \tag{221}$$

Plugging the different components of the polarization tensor P_{ab} and changing the derivative with respect to θ to the derivative with respect to μ yields

$$\frac{1}{2}\Big\{\sin^2\theta Q_{,\mu\mu} + 2U_{,\mu\phi} - \frac{Q_{,\phi\phi}}{\sin^2\theta} - 4\mu Q_{,\mu} - \frac{2\mu U_{,\phi}}{\sin^2\theta} - \frac{Q}{\sin^2\theta} + \frac{\mu^2 Q}{\sin^2\theta} - Q\Big\} \tag{222}$$

From eq. 56 and 58 it follows that

$$Q(\theta,\phi) = \frac{T_0}{4}\sum_l (2l+1)P_l(\cos\theta)(1+\cos^2\theta)\cos 2\phi\beta_l \tag{223}$$

$$U(\theta,\phi) = \frac{T_0}{4}\sum_l (2l+1)P_l(\cos\theta)2\cos\theta\sin 2\phi\beta_l. \tag{224}$$

Taking these expansions and performin the derivations on ϕ gives

$$\begin{aligned} &\frac{T_0}{8}\sum_l (2l+1)\beta_l\cos 2\phi\Big\{(1-\mu^2)[(1+\mu^2)P_l]_{,\mu\mu} - 4\mu[(1+\mu^2)P_l]_{,\mu} \\ &+\left(\frac{3-\mu^2}{1-\mu^2} - q\right)[(1+\mu^2)P_l] + 8[\mu P_l]_{,\mu} - \frac{8\mu}{1-\mu^2}[\mu P_l]\Big\} \\ &= \frac{T_0}{8}\sum_l (2l+1)\beta_l\cos 2\phi \\ &\times\Big\{(1-\mu^2)(1+\mu^2)P_{l,\mu\mu} + 8\mu(1-\mu^2)P_{l,\mu} + 12(1-\mu^2)P_l\Big\} \end{aligned}$$

$$= \frac{T_0}{8}\sum_l (2l+1)\beta_l \cos 2\phi$$
$$\times\Big\{(1+\mu^2)P_l^2 - 8\mu(1-\mu^2)^{1/2}P_l^1 + 12(1-\mu^2)P_l^0\Big\}. \quad (225)$$

In the last equality P_l was transformed into P_l^m by [7]

$$P_l^m(\mu) = (-1)^m(1-\mu^2)^{m/2}\frac{d^m P_l}{d\mu^m}. \quad (226)$$

Continuing by using the two recurrence relations [7]

$$(2l+1)\mu P_l^m = (l-m+1)P_{l+1}^m + (l+m)P_{l-1}^m \quad (227)$$

$$-(2l+1)(1-\mu^2)^{1/2}P_l^m = P_{l+1}^{m+1} - P_{l-1}^{m+1} \quad (228)$$

leads to

$$\frac{T_0}{8}\sum_l \beta_l \cos 2\phi$$
$$\times\Bigg\{P_{l+2}^2\left[\frac{l(l-1)+8l+12}{2l+3}\right]$$
$$+P_l^2\left[2l+1+\frac{(l-1)(l+3)+8(l+3)-12}{2l+3}+\frac{(l+2)(l-2)-8(l-2)-12}{2l-1}\right]$$
$$+P_{l+2}^2\left[\frac{(l+2)(l+1)-8(l+1)+12}{2l-1}\right]\Bigg\}$$
$$= \frac{T_0}{8}\sum_l \beta_l \cos 2\phi\Big\{A_l P_{l+2}^2 + B_l P_l^2 C_l P_{l+2}^2\Big\} \quad (229)$$

where the last step defines A_l, B_l and C_l. Rewriting $\cos 2\phi$ in exponential form, defining

$$D_l = \sqrt{\frac{4\pi}{2l+1}\frac{(l+2)!}{(l-2)!}} \quad (230)$$

and transforming the Legendre polynomials into spherical harmonics results in

$$P_{ab}^{\ :ab} = \frac{T_0}{16}\sum_l \beta_l\Big\{A_l D_{l+2}\left(Y_{(l+2,2)} + Y_{(l+2,-2)}\right) + B_l D_l\left(Y_{(l,2)} + Y_{(l,-2)}\right)$$
$$+C_l D_{l-2}\left(Y_{(l-2,2)} + Y_{(l-2,-2)}\right)\Big\}. \quad (231)$$

Going back to eq. 219 to calculate $a_{(lm)}^G$,

$$a_{(lm)}^G = \frac{N_l}{T_0}\int d\hat{n} Y_{(lm)}^* P_{ab}^{\ :ab}$$

$$
\begin{aligned}
&= \frac{N_l}{16}\sum_{l'}\beta_{l'} \\
&\quad \times\Big\{A_{l'}D_{l'+2}\int d\hat{n}Y^*_{(lm)}\left(Y_{(l+2,2)}+Y_{(l+2,-2)}\right) \\
&\quad +B_{l'}D_{l'}\int d\hat{n}Y^*_{(lm)}\left(Y_{(l,2)}+Y_{(l,-2)}\right) \\
&\quad C_{l'}D_{l'-2}\int d\hat{n}Y^*_{(lm)}\left(Y_{(l-2,2)}+Y_{(l-2,-2)}\right)\Big\}. \qquad (232)
\end{aligned}
$$

The orthogonality property of the spherical harmonics [6]

$$\int d\hat{n}Y^*_{(lm)}Y_{(l'm')} = \delta_{l,l'}\delta_{m,m'} \qquad (233)$$

will reduce the sum of l and force $m = \pm 2$.

$$
\begin{aligned}
a^G_{(lm)} &= \frac{1}{8}(\delta_{m,2}+\delta_{m,-2})\sqrt{\frac{2\pi}{2l+1}}\left[A_{l-2}\beta_{l-2}+B_l\beta_l+C_{l+2}\beta_{l+2}\right] \\
&= \frac{1}{8}(\delta_{m,2}+\delta_{m,-2})\sqrt{\frac{2\pi}{(2l+1)}}\left[\frac{(l+2)(l+1)\beta_{l-2}}{(2l-1)}\right. \\
&\quad \left.+\frac{6(l-1)(2l+1)(l+2)\beta_l}{(2l+3)(2l-1)}+\frac{l(l-1)\beta_{l+2}}{(2l+3)}\right] \qquad (234)
\end{aligned}
$$

A.6.2 The Magnetic Type

$$
\begin{aligned}
P_{ab}{}^{:ac}\epsilon_c{}^b &= P^{ab}_{\ :ac}\epsilon^c{}_c \\
&= \sin\theta P^{\theta\phi}_{\ \ ,\theta\theta}+\sin\theta P^{\phi\phi}_{\ \ ,\phi\theta}-\frac{P^{\theta\theta}_{\ \ ,\theta\phi}}{\sin\theta}-\frac{P^{\phi\theta}_{\ \ ,\phi\phi}}{\sin\theta}-\frac{\cos\theta}{\sin^2\theta}P^{\theta\theta}_{\ \ ,\phi} \\
&\quad +5\cos\theta P^{\theta\phi}_{\ \ ,\theta}+3\cos\theta P^{\phi\phi}_{\ \ ,\phi}+\frac{3\cos^2\theta}{\sin\theta}P^{\theta\phi}-3\sin\theta P^{\theta\phi} \\
&= \frac{1}{2}\Big\{-U_{,\theta\theta}-\frac{2Q_{,\theta\phi}}{\sin\theta}+\frac{U_{,\phi\phi}}{\sin^2\theta}-\frac{3\cos\theta}{\sin\theta}U_{,\theta} \\
&\quad -\frac{2\cos\theta}{\sin^2\theta}Q_{,\phi}+2U\Big\} \\
&= \frac{T_0}{8}\sum_l(2l+1)\sin 2\phi\beta_l \\
&\quad \times\big\{-2\mu(1-\mu^2)P_{l,\mu\mu}+-8(1-\mu^2)P_l,\mu\big\} \\
&= \frac{T_0}{4}\sum_l(2l+1)\sin 2\phi\beta_l \\
&\quad \times\big\{-\mu P^2_l+4(1-\mu^2)^{1/2}P^1_l\big\} \\
&= \frac{T_0}{4}\sum_l\beta_l\sin 2\theta\big\{(l+3)P^2_{l+1}-(l-2)P^2_{l-1}\big\}
\end{aligned}
$$

$$= \frac{iT_0}{8}\sum_l \beta_l \Big\{ (l+3)D(l+1)\left(Y_{(l+1,2)} - Y_{(l+1,-2)}\right) + (l+2)D(l-1)\left(Y_{(l-1,2)} - Y_{(l-1,-2)}\right) \Big\} \quad (235)$$

Thus calculating $a^G_{(lm)}$ from eq. 220

$$\begin{aligned} a^C_{(lm)} &= \frac{N_l}{T_0}\int d\hat{n} Y^*_{(lm)} P_{ab}{}^{:ac}\epsilon_c{}^b \\ &= \frac{iN_l}{8}\sum_{l'}\beta_{l'}\Big\{(l'+3)D_{l'+1}\int d\hat{n}Y^*_{(lm)}\left(Y_{(l'+1,2)} - Y_{(l'+1,-2)}\right) \\ &\quad +(l'-2)D_{l'-1}\int d\hat{n}Y^*_{(lm)}\left(Y_{(l'-1,2)} - Y_{(l'-1,-2)}\right)\Big\} \\ &= \frac{iN_l}{8}(\delta_{m,2}-\delta_{m,-2})\sum_{l'}\beta_{l'}\left\{(l'+3)D_{l'+1}\delta_{l,l'+1} + (l'-2)D_{l'-1}\delta_{l,l'-1}\right. \\ &= \frac{i}{4}(\delta_{m,2}-\delta_{m,-2})\sqrt{\frac{2\pi}{2l+1}}[(l+2)\beta_{l-1} + (l-1)\beta_{l+1}] \end{aligned} \quad (236)$$

$$Y^*_{(lm)} = (-1)^m Y_{(l,-m)} \quad (237)$$

$$P_{(l,-m)} = (-1)^m \frac{(l-m)!}{(l+m)!}P_{(lm)} \quad (238)$$

$$Y^*_{(lm)}(\theta,\phi) = \sqrt{\frac{(2l+1)}{4\pi}\frac{(l-m)!}{(l+m)!}}P_{(lm)}(\cos\theta)e^{-im\phi} \quad (239)$$

$$\partial^n_\phi Y^*_{(lm)} = (-im)^n Y^*_{(lm)} \quad (240)$$

A.7 Solution to RGWs Equation of Motion

In the sudden transition approximation the solution of eq. 76 is divided into three parts, for the three different eras of our universe. Since the time development of $h(\eta)$ is interesting primarly at the time of decoupling, η_d, only the solution during the first two epochs is needed.

A.7.1 Radiation Era

During the radiation era, the scale factor from eq. 261,

$$a(\eta) = a_r\eta, \quad (241)$$

gives the equation of motion for a RGW, eq. 76,

$$\ddot{h} + \frac{2}{\eta}\dot{h} + k^2 h(\eta) = 0. \quad (242)$$

Multiplying by η^2 gives

$$\eta^2\ddot{h} + 2\eta\dot{h} + \eta^2 k^2 h(\eta) = 0, \tag{243}$$

which is the radial part of Helmholtz equation with $n = 0$. The solution is then on the form of spherical Bessel and Neumann functions. The Neumann solution must be discarded because it can not fulfill the initial condition, eq. 77, since $y_0(k\eta)$ tends towards minus infinity when $k\eta$ approach zero, and the solution is

$$h(\eta) = A_0 j_0(k\eta). \tag{244}$$

A_0 is determined from the initial condition eq. 78,

$$h(\eta = 0) = A_0 = |h(k)| = \left(\frac{2\pi}{k^3} A_T \left(\frac{k}{k_0}\right)^{n_T}\right)^{1/2}. \tag{245}$$

A.7.2 Matter Era

In the matter dominated universe the scale factor is, eq. 263 approximately

$$a(\eta) = a_m \eta^2, \tag{246}$$

leading to an equation of motion

$$\eta^2\ddot{h} + 4\eta\dot{h} + \eta^2 k^2 h(\eta) = 0. \tag{247}$$

Setting $g = \eta h$ give

$$\eta^2\ddot{g} + 2\eta g + (\eta^2 k^2 - 2)g = 0 \tag{248}$$

which can be identified as the radial part of Helmholtz equation with $n = 1$ with the solution

$$g(\eta) = A_1 j_1(k\eta) + A_2 y_1(k\eta). \tag{249}$$

Substituting g for ηh and the solution in the matter dominated era is

$$h(\eta) = \frac{1}{\eta}\left(A_1 j_1(k\eta) + A_2 y_1(k\eta)\right). \tag{250}$$

The constants A_1 and A_2 are determined by fitting the two solutions, for the different eras, together at η_e. i.e. demanding the function and the first derivative to be continuous. The solutions are

$$h(\eta) = A_0 j_0(k\eta),\ \eta \geq \eta_e \tag{251}$$

$$h(\eta) = A_0 \left(\frac{\eta_e}{\eta}\right)\left[A_1 j_1(k\eta) + A_2 y_1(k\eta)\right],\ \eta_e < \eta \leq \eta_E \tag{252}$$

with the time derivatives

$$\dot{h}(\eta) = A_0 \frac{d}{d\eta} j_0(k\eta),\ \eta \geq \eta_e \tag{253}$$

$$\dot{h}(\eta) = -A_0 \left(\frac{\eta_e^2}{\eta}\right)\left[A_1 j_1(k\eta) + A_2 y_1(k\eta)\right] + A_0 \left(\frac{\eta_e}{\eta}\right)\left[A_1 \dot{j}_1(k\eta) + A_2 \dot{y}_1(k\eta)\right],\ \eta_e < \eta \leq \eta_E. \tag{254}$$

At $\eta = \eta_e$

$$\begin{aligned} j_0(k\eta_e) &= A_1 j_1(k\eta_e) + A_2 y_1(k\eta_e) \\ \dot{j}_0(k\eta_e) &= A_1 \dot{j}_1(k\eta_e) + A_2 \dot{y}_1(k\eta_e) - \frac{1}{\eta_e}\left((A_1 j_1(k\eta_e) + A_2 y_1(k\eta_e)\right). \end{aligned} \quad (255)$$

The spherical Bessel functions are

$$j_0(k\eta) = \frac{\sin(k\eta)}{k\eta} \quad (256)$$

$$j_1(k\eta) = \frac{\sin(k\eta)}{k^2\eta^2} - \frac{\cos(k\eta)}{k\eta} \quad (257)$$

$$y_1(k\eta) = -\frac{\cos(x\eta)}{k^2\eta^e} - \frac{\sin(k\eta)}{k\eta}. \quad (258)$$

After some algebra the constants are

$$\begin{aligned} A_2 &= \frac{\dot{j}_0 j_1 - j_0 \dot{j}_1 + (1/\eta_e) j_0 j_1}{\dot{y}_1 j_1 - y_1 \dot{j}_1} \\ &= \frac{2 - 2\cos(2k\eta_e) - k\eta_e \sin(2k\eta_e) - 2k^2\eta_e^2}{2k^2\eta_e^2} \end{aligned} \quad (259)$$

and

$$\begin{aligned} A_1 &= \frac{j_0 - A_2 y_1}{j_1} \\ &= \frac{3k\eta_e - k\eta_e \cos(2k\eta_e) + 2\sin(2k\eta_e)}{2k^2\eta_e^2}. \end{aligned} \quad (260)$$

A.8 Sudden Transition Approximation

Solving eq. 80 in the sudden transition approximation. In the radiation era $\eta \leq \eta_e$,

$$\dot{a}^2 = H_0^2 \Omega_r a(\eta) \Rightarrow a(\eta) = H_0 \sqrt{\Omega_r}\eta + A \quad (261)$$

where $A = 0$ to make $a(0) = 0$. The time of radiation/matter equality is then

$$\eta_e = \frac{a_e}{H_0\sqrt{\Omega_r}}, \quad (262)$$

where $a_e = \Omega_r/\Omega_m$.

At the time of matter domination

$$\dot{a}^2 = H_0^2 a \Omega_m \Rightarrow a(\eta) = \left(\frac{H_0\sqrt{\Omega_m}}{2}\eta + B\right)^2. \quad (263)$$

B can be determined with fitting the two solutions together,

$$B = \sqrt{H_0\sqrt{\Omega_r}\eta_e} - \frac{1}{2} H_0 \sqrt{\Omega_m}\eta_e \quad (264)$$

At the transition between matter and dark-energy domination the conformal time is

$$\eta_E = \frac{2(\sqrt{a_E} - B)}{H_0\sqrt{\Omega_m}}, \tag{265}$$

where $a_E = (\Omega_m/\Omega_\Lambda)^{1/2}$.

When the universe is dominated by dark energy Ω_Λ

$$a = \frac{1}{C - H_0\sqrt{\Omega_\Lambda}\eta} \tag{266}$$

where the constant C can be determined by fitting the solutions for the matter and energy eras together,

$$C = \frac{1}{\frac{1}{2}H_0\sqrt{\Omega_m}(\eta_E - \eta_e) + \sqrt{H_0\sqrt{\Omega_r}\eta_e}} + H_0\sqrt{\Omega_\Lambda}\eta_E. \tag{267}$$

To determine the present time η_0 the normalization of $a(\eta_0) = 1$ is used, i.e.

$$\eta_0 = \frac{C - 1}{H_0\sqrt{\Omega_\Lambda}} \tag{268}$$

A.9 Tight Coupling Expansion

Expanding the set of equations, eq 110-113, in the small parameter $1/q$ by defining $\epsilon = 1/q$ thus q is of order 1, while k and $\dot{h}$ is of order ϵ. With the anzats

$$\xi_l = \sum_n \xi_l^{(n)}\epsilon^n, \tag{269}$$

and

$$\beta_l = \sum_n \beta_l^{(n)}\epsilon^n. \tag{270}$$

The time evolution is then

$$\dot{\xi}_l = \sum_n \dot{\xi}_l^{(n)}\epsilon^n, \tag{271}$$

and

$$\dot{\beta}_l = \sum_n \dot{\beta}_l^{(n)}\epsilon^n. \tag{272}$$

A.9.1 Zero Order

To zero order in ϵ

$$\dot{\xi}_l^{(0)} = -q\xi_l^{(0)},\ l \geq 0, \tag{273}$$

$$\dot{\beta}_0^{(0)} = -\frac{3}{10}q\beta_0^{(0)} - \frac{1}{10}q\xi_0^{(0)} + q\left(\frac{3}{35}\beta_4^{(0)} + \frac{5}{7}\beta_2^{(0)} - \frac{3}{70}\xi_4^{(0)} + \frac{1}{7}\xi_2^{(0)}\right) \tag{274}$$

and

$$\dot{\beta}_l^{(0)} = -q\beta_l^{(0)},\ l \geq 1. \tag{275}$$

Since the radiation initially is unperturbed, $\xi(0) = \beta(0) = 0$,

$$\xi_l^{(0)} = \beta_l^{(0)} = 0,\ l \geq 0 \tag{276}$$

and therefore, to zero order in ϵ

$$\xi_l(\eta) = \beta_l(\eta) = 0. \tag{277}$$

A.9.2 First Order

To first order in ϵ

$$\begin{aligned} \dot{\xi}_0^{(1)} &= -q\xi_0^{(1)} + \dot{h}, \\ \dot{\xi}_l^{(1)} &= -q\xi_l^{(1)},\ l \geq 1 \end{aligned} \tag{278}$$

and

$$\begin{aligned} \dot{\beta}_0^{(1)} &= -\frac{3}{10}q\beta_0^{(1)} - ik\beta_1^{(0)} - \frac{1}{10}q\xi_0^{(1)} + q\left(\frac{3}{35}\beta_4^{(0)} + \frac{5}{7}\beta_2^{(0)} - \frac{3}{70}\xi_4^{(0)} + \frac{1}{7}\xi_2^{(0)}\right), \\ \dot{\beta}_l^{(1)} &= -q\beta_l^{(1)} - \frac{ik}{2l+1}\left(l\beta_{l-1}^{(0)} + (l+1)\beta_{l+1}^{(0)}\right). \end{aligned} \tag{279}$$

Since the radiation initially is unperturbed, $\xi(0) = \beta(0) = 0$,

$$\xi_l^{(1)} = \beta_l^{(1)} = 0\ l \geq 1. \tag{280}$$

Together with eq. 276 this leaves

$$\begin{aligned} \dot{\xi}_0^{(1)} &= -q\xi_0^{(1)} + \dot{h}, \\ \dot{\beta}_0^{(1)} &= -\frac{3}{10}q\beta_0^{(1)} - \frac{1}{10}q\xi_0^{(1)}, \end{aligned} \tag{281}$$

and therefore, to first order in ϵ

$$\dot{\xi}_0 + q\xi_0 = \dot{h}, \tag{282}$$

$$\dot{\beta}_0 + \frac{3}{10}q\beta_0 = -\frac{1}{10}q\xi_0, \tag{283}$$

$$\xi_l = \beta_l = 0,\ l \geq 1. \tag{284}$$

A.9.3 Second Order

To second order in ϵ the ξ_l equations are

$$\begin{aligned} \dot{\xi}_0^{(2)} &= -q\xi_0^{(2)} - ik\xi_1^{(1)}, \\ \dot{\xi}_1^{(2)} &= -q\xi_1^{(2)} - \frac{ik}{3}\left(\xi_0^{(1)} + 2\xi_2^{(1)}\right), \\ \dot{\xi}_l^{(2)} &= -q\xi_l^{(2)} - \frac{ik}{2l+1}\left(\xi_{l-1}^{(1)} + 2\xi_{l+1}^{(1)}\right),\ l \geq 2. \end{aligned} \tag{285}$$

Since the radiation initially is unperturbed, $\xi(0) = 0$,

$$\xi_l^{(2)} = 0,\ l \geq 2. \tag{286}$$

Combining this with eq. 280 the second order equations are

$$\begin{aligned} \dot{\xi}_0^{(2)} &= -q\xi_0^{(2)}, \\ \dot{\xi}_1^{(2)} &= -q\xi_1^{(2)} - \frac{ik}{3}\xi_0^{(1)}, \end{aligned} \tag{287}$$

and therefore, to second order in ϵ

$$\dot{\xi}_0 = -q\xi_0 - ik\xi_1 + \dot{h}, \tag{288}$$

$$\dot{\xi}_1 = -q\xi_1 - \frac{ik}{3}\xi_0, \tag{289}$$

$$\xi_l = 0,\ l \geq 2. \tag{290}$$

B Second Order Approximation

In the second order of the tight coupling approximation article [1] claims to find an extra damping factor, $\exp(i\int q d\eta)$, independent of wavenumber, k. This section will first redo their derivations and then solve the second approximation exactly. Comparing these solutions to the one obtained in the first order approximation one realizes that there is no such extra damping. In the exact solution there is an extra damping from a cosine term but the effect of this one will not give the damping described in [1].

The first order of the tight coupling would result in a slightly different integral in eq. 135 giving a numerical factor of $\frac{1}{16\pi}\left(\frac{1}{7}\ln\frac{10}{3}\right)^2$.

To get the damping caused by photon diffusion on smaller scales the second order of $1/q$ is needed. Meaning that the fact that ξ_1 differs, from zero because of the ξ_0 term in it's equation, has to be included.

$$\dot{\xi}_0 = -q\xi_0 - ik\xi_1 + \dot{h} \tag{291}$$

$$\dot{\xi}_1 = -q\xi_1 - \frac{ik}{3}\xi_0 \tag{292}$$

$$\xi_l = 0,\ l \geq 2 \tag{293}$$

Setting

$$\xi_0 = C_0 e^{i\int \omega d\eta} \Rightarrow \dot{\xi}_0 = C_0 i\omega e^{i\int \omega d\eta} \tag{294}$$

and

$$\xi_1 = C_1 e^{i\int \omega d\eta} \Rightarrow \dot{\xi}_1 = C_1 i\omega e^{i\int \omega d\eta} \tag{295}$$

and ignoring the variations of ω on the expansion scale $\dot{a}/a$. Plugging this into eq. 291 and eq. 292 yields

$$C_0 i\omega e^{i\int \omega d\eta} = -qC_0 e^{i\int \omega d\eta} - ikC_1 e^{i\int \omega d\eta} + \dot{h} \tag{296}$$

and

$$C_1 i\omega e^{i\int \omega d\eta} = -qC_1 e^{i\int \omega d\eta} - \frac{ik}{3} C_0 e^{i\int \omega d\eta} \tag{297}$$

Ignoring $\dot{h}$ which is close to zero at low frequency gives

$$i\omega = -q - \frac{C_1}{C_0} ik \tag{298}$$

and

$$i\omega = -q - \frac{C_0}{3C_1} ik \tag{299}$$

which implies that

$$\frac{C_1}{C_0} = \pm \frac{1}{\sqrt{3}} \tag{300}$$

and then

$$\omega = iq \pm \frac{k}{\sqrt{3}} \tag{301}$$

This shows that ξ_0 will get an extra damping factor (compared to the tight-coupling limit), $e^{-\int q d\eta}$ independent of wavenumber k [1].

Solving the second order approximation exactly,

$$\begin{pmatrix} \dot{\xi}_0 \\ \dot{\xi}_1 \end{pmatrix} = \begin{pmatrix} -q & -ik \\ -ik/3 & -q \end{pmatrix} \begin{pmatrix} \xi_0 \\ \xi_1 \end{pmatrix} + \begin{pmatrix} \dot{h} \\ 0 \end{pmatrix} = A \begin{pmatrix} \xi_0 \\ \xi_1 \end{pmatrix} + \begin{pmatrix} \dot{h} \\ 0 \end{pmatrix}. \tag{302}$$

The eigenvalues to the matrix are

$$\begin{aligned} \lambda_1 &= -q - \frac{ik}{\sqrt{3}} \\ \lambda_2 &= -q + \frac{ik}{\sqrt{3}}, \end{aligned} \tag{303}$$

with eigenvectors

$$v_1 = \begin{pmatrix} 1 \\ \frac{1}{\sqrt{3}} \end{pmatrix} \quad v_2 = \begin{pmatrix} 1 \\ \frac{-1}{\sqrt{3}} \end{pmatrix}. \tag{304}$$

Defining the matrix

$$R = \begin{pmatrix} 1 & 1 \\ \frac{1}{\sqrt{3}} & \frac{-1}{\sqrt{3}} \end{pmatrix} \tag{305}$$

allow us to express $\xi_{0,1}$ in the base where A is diagonalized,

$$\begin{pmatrix} \xi_0 \\ \xi_1 \end{pmatrix} = R \begin{pmatrix} \psi_0 \\ \psi_1 \end{pmatrix}. \tag{306}$$

The differential equations decouple

$$\begin{pmatrix} \dot{\psi_0} \\ \dot{\psi_1} \end{pmatrix} = R^{-1}AR \begin{pmatrix} \psi_0 \\ \psi_1 \end{pmatrix} + R^{-1} \begin{pmatrix} \dot{h} \\ 0 \end{pmatrix} \tag{307}$$

and can be solved separately

$$\psi_0 = \int_0^{\eta_0} \frac{\dot{h}}{2}(\eta')e^{-\kappa(\eta_0,\eta')}e^{-\frac{ik}{\sqrt{3}}(\eta'-\eta_0)}d\eta' \tag{308}$$

$$\psi_1 = \int_0^{\eta_0} \frac{\dot{h}}{2}(\eta')e^{-\kappa(\eta_0,\eta')}e^{\frac{ik}{\sqrt{3}}(\eta'-\eta_0)}d\eta'. \tag{309}$$

Transforming back to the original base

$$\xi_0 = \psi_0 + \psi_1 = \int_0^{\eta_0} \dot{h}(\eta')e^{-\kappa(\eta_0,\eta')}\cos\left(\frac{k}{\sqrt{3}}(\eta'-\eta_0)\right)d\eta', \tag{310}$$

and the soluction to the first order approximation is

$$\xi_0 = \int_0^{\eta_0} \dot{h}e^{-\kappa(\eta)}d\eta = \int_0^{\eta_0} \dot{h}e^{-\int q(\eta')d\eta'}d\eta. \tag{311}$$

Instead of the k independent damping factor we can see an extra $\cos\frac{k}{\sqrt{3}}(\eta'-\eta_0)$ in the exact solution to the second order approximation.

References

[1] W. Zhao and Y. Zhang, Phys. Rev. D **74**, 083006 (2006).

[2] P. Cabella and M. Kamionkowski, astro-ph/0403392v2 (2005).

[3] B.G. Keating, A.G. Polnarev, N.J. Miller and D. Baskaran, Int. J. Mod. Phys. A **21**, 2459-2479 (2006).

[4] B.F. Schutz, *A first course in general relativity* (Cambridge University Press, Cambridge, UK, 1985).

[5] M. Kamionkowski, A. Kosowsky and A. Stebbins, Phys. Rev. D **55**, 7368-7388 (1996).

[6] G.B. Arfken and H.J. Weber, *Mathematical methods for physicists* (Elsevier Academic Press, USA, 2005).

[7] M. Abramowitz and I.A. Stegun, *Handbook of mathematical functions* (Dover Publications, INC., New York, 1972).

[8] M. Kamionkowski, A. Kosowsky and A. Stebbins, Phys. Rev. D **55**, 061597 (1997).

[9] J.R. Pritchard and M. Kamionkowski, Ann. Phys. **318**, 2 (2005).

[10] D.N. Spergel, R. Bean, O. Dore', M.R. Nolta, C.L. Bennett, G. Hinshaw, N. Jarosik, E. Komatsu, L. Page, H.V. Peiris, L. Verde, C. Barnes, M. Halpern, R.S. Hill, A. Kogut, M. Limon, S.S. Meyer, N. Odegard, G.S. Tucker, J.L. Weiland, E. Wollack and E.L. Wright, Astrophys. J. Suppl. 170:337 (2007).

[11] L. Page, G. Hinshaw, E. Komatsu, M.R. Nolta, D.N. Spergel, C.L. Bennett, C. Barnes, R. Bean, O. Dore', M. Halpern, R.S. Hill, N. Jarosik, A. Kogut, M. Limon, S.S. Meyer, N. Odegard, H.V. Peiris, G.S. Tucker, L. Verde, J.L. Weiland, E. Wollack and E.L. Wright, Astrophys. J. Suppl. 170:335 (2007).

[12] H-U. Bengtsson, *Om klassisk fysik* (Glerups förlag, Malmö, Swe, 1995).

[13] C. Nordling and J. Österman, *Physics Handbook* (Studentlitteratur, Lund, Swe, 2004).

[14] A. Persson and L-C. Böiers, *Analys i flera variabler* (Studentlitteratur, Lund, Swe, 1988).

[15] M. Rowan-Robinson, *Cosmology* (Clarendon Press, Oxford, 2004).

[16] K.W. Ng and A.D. Speliotopoulos, Phys. Rev. D **52**, 2112-2117 (1995).

[17] M. Zaldarriaga and D.D. Harari, Phys. Rev. D **52**, 3276-3287 (1995)

[18] R.K. Sachs and A.M. Wolfe, Astrophys. J. **445**, 521 (1995).

[19] A. Polnarev, Sov. Astron. **29**, 6 (1985).

[20] http://www.wikipedia.org.

[21] http://bolo.berkeley.edu/∼yuki/CMBpol/CMBpol.htm.

[22] http://www.rssd.esa.int/index.php?project=Planck.

[23] http://map.gsfc.nasa.gov/index.html.